Regional variability in the vertical flux of particulate organic carbon in the ocean interior

Michael Lutz
Department of Geological and Environmental Science, Stanford University, Stanford, California, USA
Climate System Modeling Group, Lawrence Livermore National Laboratory, Livermore, California, USA

Robert Dunbar
Department of Geological and Environmental Science, Stanford University, Stanford, California, USA

Ken Caldeira
Climate System Modeling Group, Lawrence Livermore National Laboratory, Livermore, California, USA

Received 11 December 2000; revised 21 June 2001; accepted 27 June 2001; published XX Month 2002.

[1] Carbon transport within sinking biogenic matter in the ocean contributes to the uptake of CO_2 from the atmosphere. Here we assess the extent to which particulate organic carbon (POC) transport to the ocean's interior can be predicted from primary production or export flux. Relationships between POC flux and depth are generally described by a uniform power law or rational decrease with depth, scaled to new or total primary production of POC. While these parameterizations of flux are used in most quantitative biogeochemical models, they are based on data sets from a limited geographic and depth range. We examine these relationships through a review of parameters derived from ^{14}C uptake experiments, regional remote sensing, ^{234}Th studies, nitrogen balances, and sediment trap records. Ocean regions considered include sites studied by the Joint Global Ocean Flux Study, Hawaii Ocean Time-Series, and Bermuda Atlantic Time-Series Study programs and involve observed and radiochemically corrected flux to depth. We demonstrate regional variability in the efficiency of the biological pump to transport organic carbon from surface waters to the ocean's interior. Commonly applied flux relationships, while representative of some areas of the ocean, generally overestimate flux to depth. We estimate that the fraction of carbon transported as POC to depths greater than 1.5 km ranges between 0.10 and 8.8% (1.1% average) of primary production and between 0.28 and 30% (5.7% average) of export from the base of the euphotic zone. We develop empirical parameterizations of flux to depth using region-specific constants. Using a one-dimensional ocean model, we predict that the residence time of biogenic carbon may vary by up to 2 orders of magnitude depending on the regional efficiency of export and vertical transport. *INDEX TERMS:* 4806 Oceanography: Biological and Chemical: Carbon cycling; 4805 Oceanography: Biological and Chemical: Biogeochemical cycles (1615); 4863 Oceanography: Biological and Chemical: Sedimentation; 4842 Oceanography: Biological and Chemical: Modeling; *KEYWORDS:* Organic carbon, primary production, export, flux, remineralization, ^{14}C, ^{234}Th, mass balance, sediment traps, *s* ratio, *p* ratio, storage

1. Introduction

[2] The flux of organic matter from surface waters to the deep ocean has a direct influence on the partitioning of CO_2 between the ocean and atmosphere. This biological carbon pump includes three interrelated processes: primary production, export, and flux to depth. Primary production in surface waters, fueled by sunlight and nutrients, converts dissolved inorganic carbon to particulate organic matter (POM) and enhances the ocean's ability to take up CO_2 from the atmosphere. POM is exported from surface waters through a variety of processes, including consumption and repackaging by zooplankton and fish into fecal pellets, particle aggregation, and zooplankton migration and excretion at depth. As exported POM sinks within the ocean's interior, mesopelagic bacteria and zooplankton oxidize the organic components back into their dissolved inorganic constituents. A small portion of sinking organic matter reaches the seafloor, where it is either remineralized, supporting benthic biological activity, or buried in the geologic record.

[3] Determining the fate of organic matter sinking below the photic zone is crucial to understanding the role of the

0886-6236/02/2000GB001383$12.00

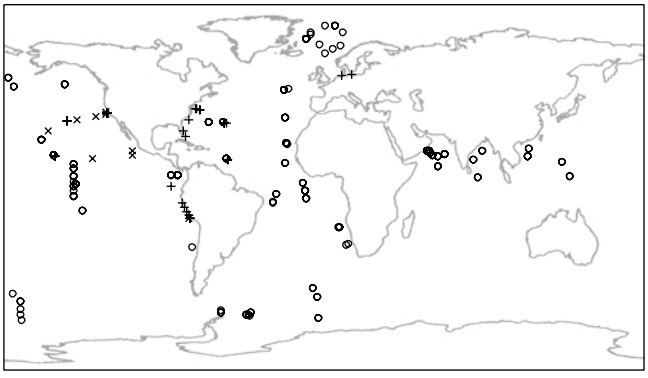

Figure 1. Locations of flux to depth measurements derived from sediment traps used in this study (open circles). The plus signs and crosses indicate the sample locations used by *Suess* [1980] and *Martin et al.* [1987], respectively. OSP, Ocean Station Papa; HOT, Hawaii Ocean Time-Series; BATS, Bermuda Atlantic Time-Series Study; NABE, North Atlantic Bloom Experiment.

biological pump in the global carbon cycle and may have a role in determining oceanic sequestration of anthropogenic CO_2, especially in the context of changing ocean circulation [*Kurz and Maier-Reimer*, 1993; *Sarmiento et al.*, 1998; *Pahlow and Riebesell*, 2000]. In general, the greater the depth at which sinking organic carbon is remineralized, the longer time it takes to return to the photic zone as dissolved CO_2, where it may reenter atmospheric carbon cycle. Organic carbon which reaches the deep ocean is entrained in water masses that have longer flow pathways back to the surface and smaller advective water velocities than in the upper ocean. The ventilation of disphotic and aphotic ocean waters occurs on timescales ranging from annual to hundreds years in the upper ocean ($\sim$0.1–1 km) to up to 1000 years in the deep ocean (>1.5 km). Thus, to describe the residence time of biogenic carbon in the ocean, the depth of remineralization must be known.

[4] The intensity of this biological pump depends on several variables, including the level of photosynthetic production, the amount of zooplankton grazing, and the degree of oxidative remineralization at different depths in the water column. Furthermore, photosynthetic production is controlled by the availability of light, nutrients, and trace metals, as well as phytoplankton speciation, temperature, and grazing. At steady state, nutrients removed from surface waters in the form of descending particulate matter are balanced by the upward advective and diffusive supply of dissolved nutrients. The upwelled nutrients support new production [*Eppley and Peterson*, 1979] in surface waters and are supplied by the remineralization of sinking organic matter.

[5] In this paper we reevaluate relationships between primary production, export, and flux to depth. We present evidence for variability in the vertical flux of organic matter within the ocean that is not accounted for by currently applied flux algorithms. We develop empirical algorithms with varied constants to predict flux to depth in different ocean regions.

2. Previous Flux to Depth Relationships

[6] The two most commonly applied descriptions of oceanic particulate organic carbon (POC) flux are that of *Suess* [1980] (equation (1)) [see also *Six and Maier-Reimer*, 1996; *Dymond et al.*, 1997; *Paerl*, 1997; *Soltwedel*, 1997; *Petsch and Berner*, 1998; *Sigman et al.*, 1998; *Tyrell*, 1999] and that of *Martin et al.* [1987] (equation (2)) [see also *Sarmiento and Le Quere*, 1996; *Brewer et al.*, 1997; *Emerson et al.*, 1997; *Druffel et al.*, 1998; *Lee et al.*, 1998; *Sarmiento et al.*, 1998; *Hedges et al.*, 1999; *Buesseler et al.*, 2000; *Fischer et al.*, 2000].

$$C_{\mathrm{flux}(z)} = \frac{C_{\mathrm{prod}}}{(0.0238z + 0.212)}, \tag{1}$$

$$C_{\mathrm{flux}(z)} = C_{\mathrm{export}}\left(\frac{z}{z_0}\right)^{-0.858}. \tag{2}$$

Flux to depth $C_{\mathrm{flux}(z)}$ is described as a function of the primary production of organic carbon in surface waters C_{prod} or the export of organic carbon C_{export} from the base of the photic zone z_0, scaled to depth below the sea surface z.

[7] The *Suess* [1980] rational equation was determined from ^{14}C-based primary production and sediment trap flux measurements, collected from the subtropical eastern Pacific and northwestern Atlantic at depths between 50 and 5400 m (Figures 1 and 2). The specific relationship between primary production and particle flux out of the

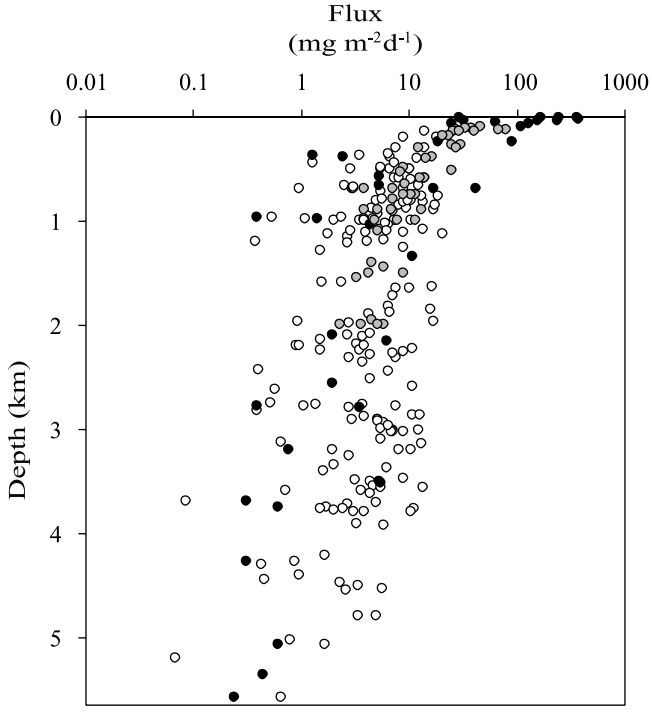

Figure 2. Global ocean annual sediment trap POC flux versus depth used by *Suess* [1980] and *Martin et al.* [1987] and in this paper (solid, shaded, and open circles, respectively; references in Table 1). Dotted horizontal lines indicate depth bins used in regional correlation analysis.

euphotic zone is unclear [*Knauer et al.*, 1984a]. The inability of primary production to predict flux in many areas [*Bishop*, 1989; *Boyd and Newton*, 1995; *Karl et al.*, 1996; *Lampitt and Antia*, 1997] suggests that the magnitude of primary production may not be the most important factor in determining flux to depth [*Boyd and Newton*, 1999]. The flux to depth relationship of *Martin et al.* [1987], based on export, is thought to be a more accurate parameterization of flux to depth [*Bishop*, 1989; *Boyd and Newton*, 1999; *Lampitt and Antia*, 1997].

[8] The *Martin et al.* [1987] normalized power function is a ''best fit'' derived from sediment trap data collected in the low-latitude to midlatitude east Pacific from depths between 100 and 2000 m (Figures 1 and 2). The exponent (-0.858) has been shown to vary within and between ocean basins [e.g., *Banse*, 1994; *Karl et al.*, 1996; *Usbeck*, 1999], suggesting that flux cannot be described by variability in export alone. However, the *Martin et al.* [1987] relationship was adopted by the Ocean Carbon Model Intercomparison Project (OCMIP) project as a component of the ''standard'' OCMIP biology model. Global ocean models commonly describe flux to depth using the fixed parameters shown in (1) and (2). The global variability of the relationships between POC flux to depth and export or primary production has not previously been assessed.

3. Methods

3.1. Data Selection

[9] We assess the ability of the currently applied *Suess* [1980] and *Martin et al.* [1987] algorithms to predict flux to depth. We apply primary production estimates predominantly derived from ^{14}C uptake experiments, and we apply export estimates derived from several methods including thorium isotope uptake experiments, *f* ratios, and mass balances. Flux predicted by the *Suess* [1980] and *Martin et al.* [1987] relationships is compared to sediment trap measurements from different ocean regions. We use the data outlined above to generate new empirical region-specific flux algorithms. The variability of ocean carbon storage predicted by the region-specific flux algorithms is assessed in a one-dimensional ocean model.

[10] Regions were selected on the basis of the availability of primary production, export, and multiple flux to depth estimates to include a variety of physical and biogeochemical provinces. Process studies include the North Atlantic Bloom Experiment (NABE), equatorial Pacific, and Arabian Sea Joint Global Ocean Flux Study (JGOFS) programs. Time series studies include those from the Sargasso Sea/Bermuda Atlantic Time-Series Study (BATS), northeast subarctic Pacific/Ocean Station Papa (OSP), and north central Pacific gyre/Hawaii Ocean Time-Series (HOT). Data selection and filtering are outlined in sections 3.2 and 3.3.

3.2. Estimating Flux to Depth Using Sediment Trap Data

[11] Problems associated with using sediment traps to characterize flux include hydrodynamic biases [*Lorenzen et al.*, 1981; *Baker et al.*, 1988; *Buesseler*, 1991; *Gust et al.*, 1992, 1994; *Siegel et al.*, 1990; *Siegel and Deuser*, 1997], zooplankton migration [*Longhurst and Harrison*, 1988; *Walsh et al.*, 1988; *Dam et al.*, 1995], sample contamination by swimmers [*Lee et al.*, 1988; *Karl and Knauer*, 1989; *Michaels et al.*, 1990], sample degradation [*Knauer et al.*, 1984b; *Honjo*, 1990; *Honjo et al.*, 1995], and brine addition [*Macintyre et al.*, 1995; *Gardner*, 2000]. Hence the accuracy of sediment traps is debated [*Jurg*, 1996; *Gust and Kozerski*, 2000]. Reported errors associated with these caveats are variable; some arguably decrease with increasing depth below the photic zone [*Gardner*, 2000].

[12] The use of sediment traps for measuring the flux of settling particles to the deep ocean (>1.5 km) has been validated by ^{230}Th and ^{231}Pa calibration studies [*Scholten et al.*, 2001; *Yu et al.*, 2001]. These radionuclide studies suggest that sediment traps may often undersample fluxes within the mesopelagic zone (<1.5 km). With the exception of the California margin, *Yu et al.* [2001] found that a trapping efficiency of 40% is a typical minimum value for the pelagic upper ocean. To account for the potential undertrapping error, we perform our analyses both with and without this correction factor applied to samples from within the mesopelagic zone. In particular, radiochemically calibrated fluxes are calculated to be the observed flux divided by 0.4. This trapping efficiency estimate may be uncertain in part because of the variable incorporation of radionuclides on particles of different sizes [*Gardner*, 2000; *Yu et al.*, 2001].

[13] Data from ocean sediment trap deployments of the past 20 years are compiled in Table 1 and Figures 1 and 2. The following criteria are used in selecting sediment trap data for this study: (1) All values are from depths greater than the local photic zone and mixed layer depth maximum, (2) data from within 200 m of the seafloor are excluded to avoid contamination by sediment resuspension, (3) sediment traps located within coastal/shelf regions (generally, total water depths <500 m) are excluded to avoid input of terrigenous organic matter, and (4) data are included only if flux to depth is measured throughout an entire year. Exceptions to criterion 4 occur occasionally where samples were collected for a periods shorter than a full year. Accordingly, taking into account seasonal bias, the calculated flux is reported as a minimum if the samples were collected during low-flux periods or as a maximum if they were collected during high-flux periods. The *Suess* [1980] and *Martin et al.* [1987] relationships are each based on less than 50 sediment trap data points, of which >80% do not meet the criteria listed above and are not included. Our analysis includes 180 new sediment trap annual flux estimates.

[14] The analytical determination of POC in sediment trap samples has been refined during the past few decades. Not all data sources (Table 1) specify the methodology used to separate particulate inorganic carbon (PIC) from POC. When methods are cited, both fuming with acid and acid rinsing are most commonly used to remove PIC. These methods may lead to the overestimations and underestimations of POC concentrations [*Grasshoff et al.*, 1999]. Conversely, the treatment method used to remove PIC may be within the error of sediment trap sample processing [*Honjo*, 1980]. While the lack of methodological consistency intro-

Table 1. Sediment-Trap-Derived Annual Flux to Depth Rates[a]

Region	Trap ID	Collection, Interval, Years	Latitude	Longitude	Water Depth, m	Trap Depth, m	POC Flux, mg m^{-2} d^{-1}	Trap Type	Reference
Polar Arctic									
Subarctic Atlantic[b]	LB-1	1983–1984	69.5	10	3161	2761	1.37	Parflux 5	*Honjo et al.* [1987]
Subarctic Atlantic[b]	BI-1	1984–1985	76	11	–	2800	2.85	Parflux 5	*Honjo et al.* [1987]
Subarctic Atlantic[b]	FS-1	1984–1985	78.9	1.4	2823	2442	0.41	Parflux 6	*Honjo et al.* [1987]
Subarctic Atlantic[b]	SP1	1987–1988	78.9	6.7	1618	1087	13.7	Kiel SMT	*Hebbeln* [2000]
Subarctic Atlantic[b]	SP2	1988–1989	78.9	6.7	1661	1110	9.0	Kiel SMT	*Hebbeln* [2000]
Subarctic Atlantic[b]	SP3	1989–1990	78.9	6.7	1676	1125	21.1	Kiel SMT	*Hebbeln* [2000]
Subarctic Atlantic[b]	NA-1	1985–1986	65.5	1	3058	2630	0.59	Parflux 6	*Honjo et al.* [1987]
Norwegian Sea[b]	–	1986–1987	67.8	5.5	1300	500	6.66	funnel	*Bathmann et al.* [1990]
Subarctic Atlantic[b]	NB-1	1985–1986	70	−2	3269	2749	0.53	Parflux 6	*Honjo et al.* [1987]
Greenland Sea[b]	OG	1988–1989	72.5	−9.5	2700	500	10.4	Kiel	*Bodungen et al.* [1995]
Greenland Sea[b]	OG	1988–1989	72.5	−9.5	2700	1000	3.56	Kiel	*Bodungen et al.* [1995]
Greenland Sea[b]	OG	1988–1989	72.5	−9.5	2700	2200	0.9	Kiel	*Bodungen et al.* [1995]
Greenland Sea[b]	OG	1989–1990	72.5	−9.5	2700	500	10.1	Kiel	*Bodungen et al.* [1995]
Greenland Sea[b]	OG	1989–1990	72.5	−9.5	2700	1000	3.86	Kiel	*Bodungen et al.* [1995]
Greenland Sea[b]	OG	1990–1991	72.5	−9.5	2700	500	2.93	Kiel	*Bodungen et al.* [1995]
Greenland Sea[b]	OG	1990–1991	72.5	−9.5	2700	1000	2.05	Kiel	*Bodungen et al.* [1995]
Greenland Sea[b]	OG	1990–1991	72.5	−9.5	2700	2200	0.99	Kiel	*Bodungen et al.* [1995]
Greenland Sea[b]	GB-21	1985–1986	74.6	−6.7	2588	1966	0.94	Parflux 5	*Honjo et al.* [1987]
Greenland Sea[b]	GB-23	1985–1986	75.6	−6.7	3445	2823	0.4	Parflux 5	*Honjo et al.* [1987]
Atlantic Ocean									
NE Atlantic[b]	–	1989–1990	47.8	−19.5	4555	3100	5.5	Parflux 7	*Newton et al.* [1994]
NABE[b]	S	1989–1990	33.8	−21	5100	1160	2.74	Parflux 7	*Honjo and Manganini* [1993]
NABE[b]	S	1989–1990	33.8	−21	5100	1980	2.82	Parflux 7	*Honjo and Manganini* [1993]
NABE[b]	S	1989–1990	33.8	−21	5100	4480	2.36	Parflux 7	*Honjo and Manganini* [1993]
NABE[b]	N	1989–1990	47.7	−21.7	4435	1110	4.05	Parflux 7	*Honjo and Manganini* [1993]
NABE[b]	N	1989–1990	47.7	−21.7	4435	2110	3.78	Parflux 7	*Honjo and Manganini* [1993]
NABE[b]	N	1989–1990	47.7	−21.7	4435	3730	2.74	Parflux 7	*Honjo and Manganini* [1993]
Sargasso Sea[b]	S_2	1977[c]	31.5	−55.9	5581	976	2.43[d]	Parflux	*Honjo* [1980]
Sargasso Sea[b]	S_2	1977[c]	31.5	−55.9	5581	3694	0.087[d]	Parflux	*Honjo* [1980]
Sargasso Sea[b]	S_2	1977[c]	31.5	−55.9	5581	5206	0.07[d]	Parflux	*Honjo* [1980]
Sargasso Sea/BATS	BATS	1988–1998	31.7	−64.2	4400	150	26.0	MultiPIT	BATS online data
Sargasso Sea/BATS	BATS	1989–1998	31.7	−64.2	4400	200	20.2	MultiPIT	BATS online data
Sargasso Sea/BATS[b]	BATS	1989–1998	31.7	−64.2	4400	300	14.1	MultiPIT	BATS online data
Sargasso Sea/BATS[b]	BATS	1989–1990	31.8	−64.2	4400	400	12.2	MultiPIT	BATS online data
Sargasso Sea[b]	SCIFF	1979–1985	31.8	−64.2	4400	3200	2.0	Parflux	*Deuser et al.* [1990]
SW Africa	NU2	–	−29	13	–	768	18.9	–	*Usbeck* [1999]
SW Africa	NU2-l	1992–1993	−28.6	14.6	3055	2516	4.4	–	*Fischer et al.* [2000]
SW Africa	WR1	1988–1989	−20.1	9.2	2217	1640	16.7	Kiel SMT	*Wefer and Fischer* [1993]
SW Africa	WR2u	1989–1990	−20	9.2	2196	599	14	Kiel SMT	*Wefer and Fischer* [1993]
SW Africa	WR2l	1989–1990	−20	9.2	2196	1654	10.4	Kiel SMT	*Wefer and Fischer* [1993]
SW Africa	WR3	1990–1991	−20	9	2208	1648	7.73	Kiel SMT	*Usbeck* [1999]
NW Africa[b]	CV1u, 2u	1992–1994	11.5	−21	4968	1000	7.36	Kiel SMT	*Usbeck* [1999]
NW Africa[b]	CV1l, 2l	1992–1994	11.5	−21	4968	4500	3.48	Kiel SMT	*Usbeck* [1999]
NW Africa[b]	CB1-l	1988–1989	20.8	−19.7	3646	2195	3.3	Parflux 6	*Fischer et al.* [1996]
NW Africa[b]	CB2-l	1989–1990	21.1	−20.7	4092	3502	4.4	Parflux 5	*Fischer et al.* [1996]
NW Africa[b]	CB3-u	1990–1991	21.1	−20.7	4094	730	5.5	Kiel SMT	*Fischer et al.* [1996]
NW Africa[b]	CB3-l	1990–1991	21.1	−20.7	4094	3557	4.7	Kiel SMT	*Fischer et al.* [1996]
NW Africa[b]	CB4-u	1991[c]	21.1	−20.7	4108	733	9.3[e]	Kiel SMT	*Fischer et al.* [1996]
NW Africa[b]	CB4-l	1991[c]	21.1	−20.7	4108	3562	5.5[e]	Kiel SMT	*Fischer et al.* [1996]
Equatorial Atlantic	WA3u	1993–1994	−7.5	−28.0	5570	671	2.6	–	*Fischer et al.* [2000]
Equatorial Atlantic	WA3l	–	−8	−28	5570	5031	0.81	–	*Usbeck* [1999]
Equatorial Atlantic	EA8u	1991–1992[c]	−5.8	−9.4	3450	598	7.45	–	*Usbeck* [1999]
Equatorial Atlantic	EA8m	1991–1992[c]	−5.8	−9.4	3450	1833	6.47	–	*Usbeck* [1999]
Equatorial Atlantic	EA8l	1991–1992[c]	−5.8	−9.4	3450	2890	3.92	–	*Usbeck* [1999]
Equatorial Atlantic	WA4u	–	−4	−26	–	808	5.1	–	*Usbeck* [1999]
Equatorial Atlantic	WA4l	–	−4	−26	–	4555	2.67	–	*Usbeck* [1999]
Equatorial Atlantic	GBZ4	1989–1990	−2.2	−9.9	3912	696	3	Kiel SMT	*Wefer and Fischer* [1993]
Equatorial Atlantic	GBZ5u	–	−2	−10	–	597	8.22	–	*Usbeck* [1999]
Equatorial Atlantic	GBZ5l	–	−2	−10	–	3382	6.3	–	*Usbeck* [1999]
Equatorial Atlantic	GBN3u	1989–1990	1.8	−11.1	4481	853	8.2	Kiel SMT	*Wefer and Fischer* [1993]
Equatorial Atlantic	GBN3l	1989–1990	1.8	−11.1	4481	3921	6	Kiel SMT	*Wefer and Fischer* [1993]
Subtropical Atlantic	E	1977–1978[c]	13.5	−54	5288	389	6.73[f]	Parflux 2	*Honjo* [1980]

Table 1. (continued)

Region	Trap ID	Collection, Interval, Years	Latitude	Longitude	Water Depth, m	Trap Depth, m	POC Flux, mg m^{-2} d^{-1}	Trap Type	Reference
Subtropical Atlantic	E	1977–1978[c]	13.5	−54	5288	988	3.94[f]	Parflux 2	*Honjo* [1980]
Subtropical Atlantic	E	1977–1978[c]	13.5	−54	5288	3755	1.73[f]	Parflux 2	*Honjo* [1980]
Subtropical Atlantic	E	1977–1978[c]	13.5	−54	5288	5068	1.7[f]	Parflux 2	*Honjo* [1980]
Pacific Ocean									
Ocean Station P	OSP	1989–1993	50	−145	4250	200	18.2	Parflux 5–7	*Wong et al.* [1999]
Ocean Station P[b]	OSP	1983–1993	50	−145	4250	1000	7.42	Parflux 5–7	*Wong et al.* [1999]
Ocean Station P[b]	OSP	1982–1993	50	−145	4250	3800	3.10	Parflux 5–7	*Wong et al.* [1999]
Subarctic Pacific[b]	Aleutian Islands	–	49	−174	5400	4800	3.4	–	*Takahashi* [1995]
Subarctic Pacific[b]	Aleutian Islands	–	49	−174	5400	4800	5.1	–	*Takahashi* [1995]
Subarctic Pacific[b]	Bering Sea	–	53.5	−177	3800	3200	8.1	–	*Takahashi* [1995]
Subarctic Pacific[b]	Bering Sea	–	53.5	−177	3800	3200	10.5	–	*Takahashi* [1995]
North central Pacific Gyre[b]	P_1	1978[c]	15.4	−152	5792	378	3.56[g]	Parflux 2	*Honjo* [1980]
North central Pacific Gyre[b]	P_1	1978[c]	15.4	−152	5792	978	0.55[g]	Parflux 2	*Honjo* [1980]
North central Pacific Gyre[b]	P_1	1978[c]	15.4	−152	5792	2778	1.09[g]	Parflux 2	*Honjo* [1980]
North central Pacific Gyre[b]	P_1	1978[c]	15.4	−152	5792	4280	0.88[g]	Parflux 2	*Honjo* [1980]
North central Pacific Gyre[b]	P_1	1978[c]	15.4	−152	5792	5582	0.66[g]	Parflux 2	*Honjo* [1980]
North central Pacific Gyre/HOT	ALOHA	1988–1999	22.8	−158.0	4800	150	14[h]	MultiPIT	HOT online data
North central Pacific Gyre/HOT	ALOHA	1994–1996	22.8	−158.0	4800	200	9[h]	MultiPIT	HOT online data
North central Pacific Gyre/HOT	ALOHA	1988–1995	22.8	−158.0	4800	300	7.7[h]	MultiPIT	HOT online data
North central Pacific Gyre/HOT[b]	ALOHA	1989–1995	22.8	−158.0	4800	500	5.5[h]	MultiPIT	HOT online data
South China Sea[b]	SCS-C	1990–1995	14.6	115.1	4310	1200	4.20	Parflux 6	*Jianfang et al.* [1998]; *Wiesner et al.* [1996]
South China Sea[b]	SCS-C	1990–1995	14.6	115.1	4310	2240	3.51	Parflux 6	*Jianfang et al.* [1998]
South China Sea[b]	SCS-C	1990–1995	14.6	115.1	4310	3770	2.52	Parflux 6	*Jianfang et al.* [1998]; *Wiesner et al.* [1996]
South China Sea[b]	SCS-N	1987–1988	18.5	116	3750	1000	3.92	Parflux 6	*Jianfang et al.* [1998]; *Wiesner et al.* [1996]
South China Sea[b]	SCS-N	1987–1988	18.5	116	3750	3350	2.02	Parflux 6	*Jianfang et al.* [1998]; *Wiesner et al.* [1996]
North Equatorial Current	NEC-T	1988–1989	12.0	134.3	5300	1200	0.38	Parflux 6	*Kempe and Knaack* [1996]
North Equatorial Current	NEC-B	1988–1989	12.0	134.3	5300	4300	0.43	Parflux 6	*Kempe and Knaack* [1996]
Equatorial Counter Current	ECC-T	1988–1989	5.0	138.8	4130	1130	1.78	Parflux 6	*Kempe and Knaack* [1996]
Equatorial Counter Current	ECC-B	1988–1989	5.0	138.8	4130	3130	0.67	Parflux 6	*Kempe and Knaack* [1996]
Equatorial Pacific[b]	S	1983–1984	11	−19140	4800	700	3.12	OSU trap	*Dymond and Collier* [1988]
Equatorial Pacific[b]	S	1983–1984	11	−140	4800	1600	2.38	OSU trap	*Dymond and Collier* [1988]
Equatorial Pacific[b]	S	1983–1984	11	−140	4800	3400	1.62	OSU trap	*Dymond and Collier* [1988]
Equatorial Pacific[b]	9N	1992–1993	9	−140	5100	2150	1.51	Parflux	*Honjo et al.* [1995]
Equatorial Pacific[b]	9N	1992–1993	9	−140	5100	2250	1.52	Parflux	*Honjo et al.* [1995]
Equatorial Pacific[b]	9N	1992–1993	9	−140	5100	4400	0.96	Parflux	*Honjo et al.* [1995]
Equatorial Pacific[b]	5N	1992–1993	5	−140	4493	1191	6.02	Parflux	*Honjo et al.* [1995]
Equatorial Pacific[b]	5N	1992–1993	5	−140	4493	2091	4.50	Parflux	*Honjo et al.* [1995]
Equatorial Pacific[b]	5N	1992–1993	5	−140	4493	3793	3.84	Parflux	*Honjo et al.* [1995]
Equatorial Pacific[b]	2N	1992–1993	2	−140	4397	2203	3.96	Parflux	*Honjo et al.* [1995]
Equatorial Pacific[b]	C	1983–1984	1	−139	4400	1095	2.96	OSU trap	*Dymond and Collier* [1988]
Equatorial Pacific[b]	C	1983–1984	1	−139	4400	1895	4.25	OSU trap	*Dymond and Collier* [1988]
Equatorial Pacific[b]	C	1983–1984	1	−139	4400	3495	3.26	OSU trap	*Dymond and Collier* [1988]
Equatorial Pacific[b]	C	1984–1985	1	−139	4400	1083	5.36	OSU trap	*Dymond and Collier* [1988]
Equatorial Pacific[b]	C	1984–1985	1	−139	4400	1883	6.78	OSU trap	*Dymond and Collier* [1988]
Equatorial Pacific[b]	C	1984–1985	1	−139	4400	2908	5.18	OSU trap	*Dymond and Collier* [1988]
Equatorial Pacific[b]	EQ	1992–1993	0	−140	4358	880	4.64	Parflux	*Honjo et al.* [1995]
Equatorial Pacific[b]	EQ	1992–1993	0	−140	4358	2284	4.49	Parflux	*Honjo et al.* [1995]
Equatorial Pacific[b]	EQ	1992–1993	0	−140	4358	3618	4.38	Parflux	*Honjo et al.* [1995]
Equatorial Pacific[b]	2S	1992–1993	−2	−140	4293	3593	3.61	Parflux	*Honjo et al.* [1995]
Equatorial Pacific[b]	5S	1992–1993	−5	−140	4198	1216	2.72	Parflux	*Honjo et al.* [1995]

Table 1. (continued)

Region	Trap ID	Collection, Interval, Years	Latitude	Longitude	Water Depth, m	Trap Depth, m	POC Flux, mg m^{-2} d^{-1}	Trap Type	Reference
Equatorial Pacific[b]	5S	1992–1993	−5	−140	4198	2099	2.72	Parflux	*Honjo et al.* [1995]
Equatorial Pacific[b]	5S	1992–1993	−5	−140	4198	2316	2.80	Parflux	*Honjo et al.* [1995]
Equatorial Pacific[b]	12S	1992–1993	−12	−135	4294	1292	1.52	Parflux	*Honjo et al.* [1995]
Equatorial Pacific[b]	12S	1992–1993	−12	−135	4294	3594	0.72	Parflux	*Honjo et al.* [1995]
Peru-Chile Current	CH-3-4	1993–1994	−30	−73.2	4360	2323	7.67	Kiel SMT	*Hebbeln et al.* [2000]
Panama Basin[b]	PB	1979[c]	5.35	−81.9	3856	667	12.6[i]	Parflux	*Honjo et al.* [1982]
Panama Basin[b]	PB	1979[c]	5.35	−81.9	3856	1268	8.95[i]	Parflux	*Honjo et al.* [1982]
Panama Basin[b]	PB	1979[c]	5.35	−81.9	3856	2265	9.06[i]	Parflux	*Honjo et al.* [1982]
Panama Basin[b]	PB	1979[c]	5.35	−81.9	3856	2869	10.9[i]	Parflux	*Honjo et al.* [1982]
Panama Basin[b]	PB	1979[c]	5.35	−81.9	3856	3769	11.4[i]	Parflux	*Honjo et al.* [1982]
Panama Basin[b]	PB	1979[c]	5.35	−81.9	3856	3791	10.6[i]	Parflux	*Honjo et al.* [1982]
Panama Basin[b]	–	1979–1980	5.37	−85.6	3860	890	9.7	Parflux 2	*Honjo* [1982]
Panama Basin[b]	–	1979–1980	5.37	−85.6	3860	2590	10.9	Parflux 2	*Honjo* [1982]
Panama Basin[b]	–	1979–1980	5.37	−85.6	3860	3560	13.7	Parflux 2	*Honjo* [1982]
Indian Ocean									
Arabian Sea, oceanic[b]	MS5	1994–1995[c]	10	65	4411	800	5.7[j]	Parflux 7	*Honjo et al.* [1999]
Arabian Sea, oceanic[b]	MS5	1994–1995	10	65	4411	2363	3.8	Parflux 7	*Honjo et al.* [1999]
Arabian Sea, oceanic[b]	MS5	1994–1995	10	65	4411	3915	3.3	Parflux 7	*Honjo et al.* [1999]
Arabian Sea, oceanic[b]	CAST	1987	14.5	64.6	3904	2913	3.0	Parflux 6	*Haake et al.* [1993]
Arabian Sea, oceanic[b]	CAST	1986	14.5	64.6	3906	2907	5.2	Parflux 6	*Haake et al.* [1993]
Arabian Sea, oceanic[b]	CAST	1988	14.5	64.6	3908	3021	7.1	Parflux 6	*Haake et al.* [1993]
Arabian Sea, oceanic[b]	EAST	1989	15.6	68.6	3807	2938	6.0	Parflux 6	*Haake et al.* [1993]
Arabian Sea, oceanic[b]	EAST	1987	15.6	68.6	3776	2772	3.8	Parflux 6	*Haake et al.* [1993]
Arabian Sea, oceanic[b]	EAST	1986	15.6	68.6	3776	2776	7.7	Parflux 6	*Haake et al.* [1993]
Arabian Sea, oceanic[b]	EAST	1990	15.6	68.6	3862	2928	5.2	Parflux 6	*Haake et al.* [1993]
Arabian Sea, coastal[b]	MS1	1994–1995	17.7	58.9	1448	808	10.5	Parflux 7	*Honjo et al.* [1999]
Arabian Sea, coastal[b]	MS1	1994–1995[c]	17.7	58.9	1448	999	10.5[k]	Parflux 7	*Honjo et al.* [1999]
Arabian Sea, coastal[b]	MS2	1994–1995	17.4	58.8	3650	828	13.5	Parflux 7	*Honjo et al.* [1999]
Arabian Sea, coastal[b]	MS2	1994–1995	17.4	58.8	3650	903	17.2	Parflux 7	*Haake et al.* [1993]
Arabian Sea, coastal[b]	MS2	1994–1995	17.4	58.8	3650	1974	17.4	Parflux 7	*Honjo et al.* [1999]
Arabian Sea, coastal[b]	MS2	1994–1995	17.4	58.8	3650	3141	13.2	Parflux 7	*Honjo et al.* [1999]
Arabian Sea, coastal[b]	MS3	1994–1995	17.2	59.6	3470	764	13.2	Parflux 7	*Honjo et al.* [1999]
Arabian Sea, coastal[b]	MS3	1994–1995	17.2	59.6	3470	858	17.5	Parflux 7	*Honjo et al.* [1999]
Arabian Sea, coastal[b]	MS3	1994–1995	17.2	59.6	3470	1857	16.3	Parflux 7	*Honjo et al.* [1999]
Arabian Sea, coastal[b]	MS3	1994–1995	17.2	59.6	3470	2871	12.8	Parflux 7	*Honjo et al.* [1999]
Arabian Sea, coastal[b]	MS4	1994–1995	15.3	61.5	3980	821	8.9	Parflux 7	*Honjo et al.* [1999]
Arabian Sea, coastal[b]	MS4	1994–1995	15.3	61.5	3980	2229	11.1	Parflux 7	*Honjo et al.* [1999]
Arabian Sea, coastal[b]	MS4	1994–1995	15.3	61.5	3980	3478	8.9	Parflux 7	*Honjo et al.* [1999]
Arabian Sea, coastal[b]	WAST	1986	16.3	60.3	4024	3023	7.1	Parflux 6	*Haake et al.* [1993]
Arabian Sea, coastal[b]	WAST	1987	16.3	60.3	4024	3036	6.9	Parflux 6	*Haake et al.* [1993]
Arabian Sea, coastal[b]	WAST	1988	16.3	60.3	4024	3034	9.0	Parflux 6	*Haake et al.* [1993]
Arabian Sea, coastal[b]	WAST	1990	16.3	60.3	4024	3016	12.3	Parflux 6	*Haake et al.* [1993]
Bay of Bengal	South-s	1987–1988	4.4	87.3	4017	1040	6.49	Parflux	*Ittekkot et al.* [1991]
Bay of Bengal	South-d	1987–1988	4.4	87.3	4017	3006	5.59	Parflux	*Ittekkot et al.* [1991]
Bay of Bengal	Central-s	1987–1988	13.2	84.4	3259	906	7.23	Parflux	*Ittekkot et al.* [1991]
Bay of Bengal	Central-d	1987–1988	13.2	84.4	3259	2282	7.15	Parflux	*Ittekkot et al.* [1991]
Bay of Bengal	North-s	1987–1988	17.4	89.6	2263	809	9.84	Parflux	*Ittekkot et al.* [1991]
Bay of Bengal	North-d	1987–1988	17.4	89.6	2263	1727	7.26	Parflux	*Ittekkot et al.* [1991]
Polar Antarctic									
ACC, Atlantic[b]	VIII-u	1992	−62.1	−40.6	3280	2453	6.62	Parflux	*Pudsey and King* [1997]
ACC, Atlantic[b]	VIII-l	1992	−62.1	−40.6	3280	3259	2.81	Parflux	*Pudsey and King* [1997]
ACC, Atlantic[b]	I-l	1990	−63.2	−42.7	3798	3777	2.07	Parflux	*Pudsey and King* [1997]
ACC, Atlantic[b]	I-u	1992	−63.2	−42.7	3793	2966	6.53	Parflux	*Pudsey and King* [1997]
ACC, Atlantic[b]	I-l	1992	−63.2	−42.7	3793	3766	1.52	Parflux	*Pudsey and King* [1997]
ACC, Atlantic[b]	II-l	1990	−63.5	−41.7	4552	4531	5.73	Parflux	*Pudsey and King* [1997]
ACC, Atlantic[b]	III-u	1990	−64	−40.9	4537	3710	5.11	Parflux	*Pudsey and King* [1997]
ACC, Atlantic	WS2-l	1987[c]	−64.9	−2.5	5000	4456	0.47[l]	Parflux	*Wefer and Fischer* [1991]
ACC, Atlantic[b]	WS3-u	1988–1989	−64.9	−2.5	5053	360	6.47	–	*Fischer et al.* [2000]
Bouvert Island[b]	BO1-u	1990–1991	−54.3	−3.4	2734	450	7.37	funnel	*Fischer et al.* [2000]
Bouvert Island	BO2-u	1987[c]	−54.3	−3.4	2965	456	1.32[m]	funnel	*Fischer et al.* [2000]
Polar Front[b]	PF1-u	1987–1988	−50.1	−5.9	3750	700	8.93	–	*Fischer et al.* [2000]
Polar Front[b]	PF3-u	1989–1990	−50.1	−5.9	3785	614	10.5	–	*Fischer et al.* [2000]
MIZ, Atlantic	KG1-u	1983–1984	−62.3	−57.5	1952	494	5.56	Parflux 6	*Fischer et al.* [2000]
MIZ, Atlantic	KG2-u	1984–1985	−62.3	−57.5	1650	693	0.99	Parflux 6	*Fischer et al.* [2000]
MIZ, Atlantic	KG3-u	1985–1986	−62.3	−57.5	1992	687	3.07	Parflux 6	*Fischer et al.* [2000]
MIZ, Atlantic	KG1-l	1983–1984	−61.3	−57.5	1952	1588	1.6[n]	funnel	*Wefer et al.* [1988]
MIZ, Pacific	MS5	1996–1997	−66.2	−170	3016	937	5.21	Parflux 6	*Honjo et al.* [2000]
ACC, Pacific	MS4	1996–1997	−63.1	−170	2886	1031	6.03	Parflux 6	*Honjo et al.* [2000]
APFZ, Pacific	MS3	1996–1997	−60.3	−170	3958	1103	6.3	Parflux 6	*Honjo et al.* [2000]

Table 1. (continued)

Region	Trap ID	Collection, Interval, Years	Latitude	Longitude	Water Depth, m	Trap Depth, m	POC Flux, mg m^{-2} d^{-1}	Trap Type	Reference
SAF, Pacific	MS2	1996–1998	−56.9	−170	4924	982	4.66	Parflux 6	*Honjo et al.* [2000]
SAF, Pacific	MS2	1996–1998	−56.9	−170	4924	4224	1.71	Parflux 6	US JGOFS online data
SAF, Pacific	MS1	1996–1997	−53.0	−175	5441	986	1.1	Parflux 6	*Honjo et al.* [2000]

[a] MIZ, marginal ice zone; SMT, Salzgitter Electronics, Kiel; OSU, Oregon State University; ACC, Antarctic Circumpolar Current; APFZ, Antarctic Polar Frontal Zone; and SAF, Subantarctic Front.
[b] Data used in regional comparisons.
[c] Sample time periods less than 1 year.
[d] Trap deployments less than an entire year: July–October (110 days), may be overestimated.
[e] Trap deployments less than an entire year: March–November (200 days), may be overestimated.
[f] Trap deployments less than an entire year: November–February (98 days), may be underestimated.
[g] Trap deployments less than an entire year: September–November (61 days), may be underestimated.
[h] POC calculated as 50% of the total particulate carbon reported based on simultaneous inorganic and organic carbon determinations of sediment trap material from the North Pacific [*Wong et al.*, 1999].
[i] Trap deployments less than an entire year: August–December (112 days), may be underestimated.
[j] Trap deployments less than an entire year: November–April (170 days), may be underestimated.
[k] Trap deployments less than an entire year: November–August (276 days), may be overestimated.
[l] Trap deployments less than an entire year: January–November (304 days), may be underestimated.
[m] Trap deployments less than an entire year: May–December (200 days), may be underestimated.
[n] POC estimated assuming that the lower trap has the same combustible flux %C as the upper trap [*Fischer et al.*, 2000; *Wefer et al.*, 1988].

duces uncertainty into the comparison of sediment trap records, this problem, as well as other trap technology uncertainties, would have also been present in the data underlying the development of the *Martin et al.* [1987] and *Suess* [1980] parameterizations.

[15] To standardize analysis between regions where the frequency of sediment trap measurements at different depths varies, formulations of new flux to depth equations incorporate data binned between depth ranges. The flux estimates at each locale are averaged within the following depth ranges: 0.5 to 1 km, 1 to 2 km, 2 to 3 km, 3 to 4 km, and >4 km. Average flux values are assigned a nominal depth of the mean depth of observations in each depth range.

3.3. Estimating Primary Production and Export

[16] Table 2 includes regional estimates of primary production and export primarily obtained during JGOFS process, time series, and other field-based studies. In most cases, primary production was equated to net photosynthesis as estimated by ^{14}C uptake experiments. The one exception is the Southern Ocean/Atlantic sector region. Here, primary production is estimated using an algorithm based on monthly climatological phytoplankton concentrations from the coastal zone color scanner (CZCS) and in situ ^{14}C-based primary productivity data from throughout the Southern Ocean [*Arrigo et al.*, 1998]. We made this exception because of the lack of ^{14}C-based primary production results for this region.

[17] Estimates of primary production based on ^{14}C uptake experiments, as in the case of sediment traps, may include errors. Estimates of primary production may differ significantly if they are derived from carbon fixed in POC or in both dissolved organic carbon (DOC) and POC [*Sakshaug et al.*, 1997]. The duration of the incubation experiment is another potential source of error. Long incubation times may yield lower carbon uptake rates than short incubations (~1 hour) because of the likelihood of the recycling of labeled carbon [*Dring and Jewson*, 1982; *Sakshaug et al.*, 1997]. The organic C to chlorophyll a ratio is highly variable and is another potential source of error [*Sakshaug et al.*, 1997]. Hence ^{14}C-based estimates of primary production may include significant uncertainties.

[18] We employ several approaches to estimate export of particulate organic carbon from surface waters on regional and annual scales: ^{234}Th, mass balances, and new production (Table 2). The ^{234}Th-based export estimates use ^{234}Th activity measurements to calculate vertical ^{234}Th fluxes, which are multiplied by the organic C to ^{234}Th ratio of sinking particulate material to quantify POC export. While this approach has been applied to a wide range of oceanographic settings [*Buesseler*, 1998] and is a preferred methodology [*Buesseler*, 1991], associated errors have not been quantified. Calculating the ^{234}Th flux involves biases and uncertainties including steady state effects, time variability, and transport terms [*Buesseler et al.*, 1992; *Wei and Murray*, 1992; *Lee et al.*, 1993; *Kim et al.*, 1999]. Additionally, estimates of the export of organic components are associated with large errors because of uncertainty in the ratio of C:^{234}Th on sinking particles [*Michaels et al.*, 1994; *VanderLoeff et al.*, 1997; *Gardner*, 2000]. Careful elemental mass balances relying on annual budgets of dissolved and particulate material may offer the most accurate estimates of export and are incorporated where available.

[19] The export of organic carbon from surface waters is often estimated using *f* ratios by equating new production with export, assuming steady state on an annual basis. The *f* ratio is the ratio of new production to total (new plus regenerated) production. We apply this approach where annual ^{234}Th and mass balance export estimates are unavailable. A significant and variable portion of total export calculated by this method may be in the form of DOC [e.g., *Quay*, 1997; *Stoll et al.*, 1996] and unsuitable for comparison to the POC flux recorded by sediment traps. At high latitudes, where DOC is a minor component of flux

Table 2. Regional Estimates of Primary Production and Particulate Organic Carbon (POC) Export From the Base to the Photic Zone[a]

Region	Latitude	Longitude	Z_0, m	f Ratio	Export, mg C m^{-2} d^{-1}	Primary Production, mg C m^{-2} d^{-1}	Reference: Export	Reference: Primary Production
Greenland and Norwegian Seas	65° to 79°	−10° to 11°	50	0.3	70[b]	240	*Bodungen et al.* [1995][c]	*Bodungen et al.* [1995][c]
NE Atlantic/NABE	34° to 48°	−21° to −22°	40	0.45	280[b]	700	*Bury et al.* [2001][d]	*Bury et al.* [2001][d]
Sargasso Sea/BATS	32°	−56° to −64°	140	–	30, 44[e]	360	*Buesseler* [1998][f]; *Michaels et al.* [1994][e,g]	*Michaels et al.* [1994][g]
Subarctic Pacific/OSP	50°	−145°	70	–	70	1000	*Charette et al.* [1999][h]	*Boyd and Harrison* [1999][h]
North Central Pacific gyre/HOT	15° to 23°	−151° to −158°	150	–	66[e]	460	*Emerson et al.* [1997][h]	*Karl et al.* [1996][h]
South China Sea	15° to 18°	115° to 116°	100	–	230	420	*Huang et al.* [1996][i]	*Huang* [1988][j]
Arabian Sea, oceanic	10° to 16°	65° to 69°	90	–	70	1000	*Buesseler et al.* [1998] (stations n11, s11, and s15)[k]	*Barber et al.* [2001] (stations n11, s11, and s15)[k]
Arabian Sea, coastal	16° to 18°	59° to 62°	65	–	130	1250	*Buesseler et al.* [1998] (stations s2, s3, s4, and s7)[k]	*Barber et al.* [2001] (stations s2, s3, s4, and s7)[k]
Equatorial Pacific (±2° latitude)	−2° to 2°	−139° to −140°	114	–	90	1035	*Murray et al.* [1996] (stations 6–10)[l]	*Murray et al.* [1996] (stations 6–10)l
Equatorial Pacific (±5° latitude)	5°, −5°	−137° to −140°	130	–	76	780	*Murray et al.* [1996] (stations 4 and 12)[l]	*Murray et al.* [1996] (stations 4 and 12)[l]
Equatorial Pacific (±9°–16° latitude)	9° to 16°, −9° to −16°	−134° to −152°	130	–	42	344	*Murray et al.* [1996] (stations 1, 2, and 15)[l]	*Murray et al.* [1996] (stations 1, 2, and 15)[l]
Panama Basin	5°	−82° to −86°	70	0.43	100[b]	230	*Bishop et al.* [1986][m]	*Bishop et al.* [1986][m]
Southern Ocean/Atlantic sector	−50° to −65°	−2° to −43°	40	0.15	60[b]	380[n]	*Sambrotto and Mace* [2000][o]	*Arrigo et al.* [1998][p]
NW Africa	12° to 21°	−20° to −21°	50	0.6	1200[b]	2000	*Jewell* [1994][q]; *Minas et al.* [1986][q]	*Huntsman and Barber* [1977][r]

[a] Export rates derived from POC/^{234}Th uptake experiments. Primary production estimates derived from ^{14}C uptake incubation experiments.
[b] Derived from f ratios (assuming that export equals primary production times f ratio).
[c] Suggested annual mean (Table 2).
[d] Monthly weighted average April–August, 32°–50°N, 20°W data compilation (Tables 6 and 7; references cited within), may be overestimated.
[e] Derived from nutrient mass balances.
[f] Average March–October, may be overestimated.
[g] Annual average 1989–1993.
[h] Suggested annual mean.
[i] Winter, may be underestimated.
[j] Average April–July, may be overestimated.
[k] Average NE Monsoon, Spring Intermonsoon, Mid-SW Monsoon, and Late-SW Monsoon periods.
[l] Average February–March and August–September (Table 5).
[m] Average summer and winter (Table 9).
[n] Derived from regional remote sensing.
[o] Average November–March, 55°–65°S, 170°W (Table 4), export may be overestimated.
[p] Annual average Weddell Sea sector, pelagic and marginal ice zone (MIZ) (Table 2).
[q] Average coastal upwelling, may be underestimated [*Jewell*, 1994].
[r] Average March–May, may be underestimated [see *Minas et al.*, 1986].

Table 3. Descriptive Statistics of Flux Rates at Different Depth Ranges in the Global Ocean[a]

Depth, km	Average	Standard Deviation	Minimum	Maximum	*N*
0.1–0.25	17.5	6.4	9.0	26.0	5
0.25–0.5	7.2	3.6	1.3	14.1	14
0.5–1	7.4	4.7	0.55	18.9	40
1–2	6.8	5.4	0.38	21.1	30
2–3	4.5	3.3	0.40	12.8	38
3–4	5.4	3.7	0.09	13.7	38
>4	2.0	1.7	0.07	5.7	15

[a] Flux rates are given in units of mg C m^{-2} d^{-1}.

and ^{234}Th-based export rates are available during only a few months, rates of POC export are derived by assuming that new production equals POC export.

4. Results and Discussion

4.1. Flux to Depth

[20] A review of the locations of annual sediment trap sites reveals large areas with little or no data (Figure 1). The Northern Hemisphere contains almost 3 times the number of flux to depth estimates as the Southern Hemisphere contains, despite having less than 40% of the global ocean area. Few sediment trap data are available from the western sides of main ocean basins. The central ocean gyres and large portions of the Southern Ocean are poorly characterized. Areas of low productivity are relatively undersampled compared to more productive coastal margins. Oligotrophic and eutrophic portions of the ocean are relatively undersampled, compared to mesotrophic areas (70% of total samples). Furthermore, the moderately productive Southern Hemisphere Subtropical Convergence (~40°S) has received little attention. Globally, the bulk of flux to depth data is from depths greater than 1 km.

[21] Annual carbon flux to depth for all global locations is shown in Figure 2. Above 1 km, global variability of annual flux to depth is more than an order of magnitude larger than below that depth (Table 3). In the intermediate and deep ocean, variability decreases with increasing depth. Here, the vertical flux of POC follows an irregular pattern of both increasing and decreasing flux with increasing depth (Table 4). In almost half of the POC flux rate change estimates the flux to deeper traps exceeds the flux observed in shallower traps in the same region. The irregular pattern may be due to a variable availability of sinking material to decomposition, differential particle sinking trajectories [*Siegel et al.*, 1990; *Siegel and Deuser*, 1997], trapping inaccuracies, or heterogeneity of particle production and export and flux to depth within the regions considered. The variability of flux to depth estimates in the intermediate and deep ocean constitutes a minor fraction of particle production and export. Most of the modification of flux to depth occurs in the upper 1 km of the water column.

[22] Where flux data are available for both the shallow and deep ocean, fluxes to depths between 0.5 and 1 km are highly correlated with fluxes to depths greater than 1 km (Figure 3). In contrast to *Yu et al.* [2001] and *Scholten et al.* [2001], these correlations suggest that sediment trap data from depths between 0.5 to 1 km may be as "valid" as those from below 1 km. The variability of upper ocean fluxes indicates that the conditions and forcings that serve to create and attenuate variability in flux to depth are concentrated within 1 km below the base of the photic zone. While sediment-trap-derived flux to depth data may be internally consistent, primary production and export are poorly correlated with flux (Table 5). This lack of correlation suggests that using primary production or export alone may not allow for accurate predictions of flux to depth.

Table 4. Average Rate of Change of the Vertical POC Flux to Depth in the Intermediate and Deep Ocean Derived From Sediment Trap Data[a]

	Percent Δ Flux km^{-1}		
	1–2 km	2–3 km	>3 km
Greenland and Norwegian Seas	−79	76	–
NE Atlantic/NABE	−3.1	63	−54
Sargasso Sea/BATS	−79[b]	−79[b]	−61
Subarctic Pacific/OSP	12[b]	12[b]	−46
North Central Pacific gyre/HOT	55	55	−16
South China Sea	−12	−38	60
Arabian Sea, oceanic	–	68	−39
Arabian Sea, coastal	41	−32	–
Equatorial Pacific (±2° latitude)	17	7.6	42
Equatorial Pacific (±5° latitude)	−24	9[c]	9[c]
Equatorial Pacific (±9°–16° latitude)	−29	−17[c]	−17[c]
Panama Basin	1.2	43	9.8
Southern Ocean, Atlantic sector	–	−45	−39
NW Africa	−46	35	−30

[a] Positive and negative values indicate the percent by which flux observed in deeper traps exceeds or lags flux at shallower traps within the depth ranges indicated.
[b] Average over 1 to 3 km range.
[c] Average over 2 to >3 km range.

4.2. Predicted Versus Observed Flux to Depth

[23] We compare observed flux to depth, derived from sediment trap data, to predicted flux to depth using the flux

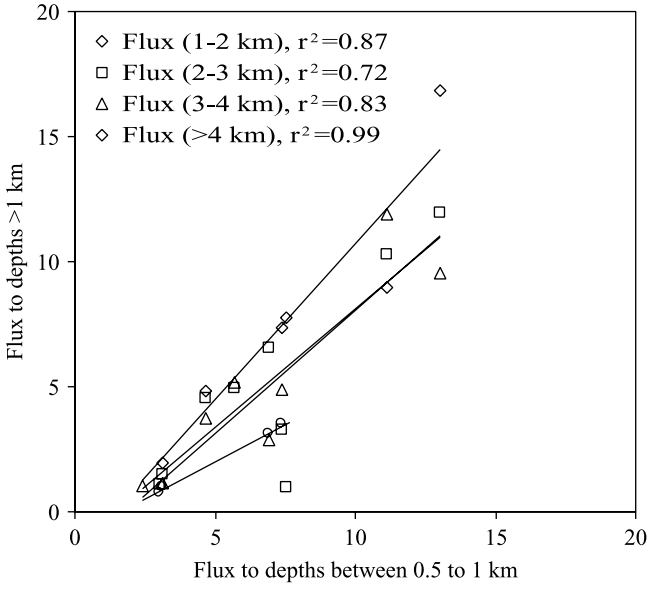

Figure 3. Relationships between sediment-trap-derived POC flux to depth estimates within different depth ranges for regions listed in Table 2.

Table 5. Correlation Matrix for Primary Production, Export From the Base of the Photic Zone (Table 2), and Flux to Various Depth Ranges (Table 1)

	Primary Production	Export	Flux (0.5–1 km)	Flux (1–2 km)	Flux (2–3 km)	Flux (3–4 km)	Flux (>4 km)
Primary production	1						
Export	0.74	1					
Flux (0.5–1 km)	0.16	0.25	1				
Flux (1–2 km)	0.03	0.32	0.93	1			
Flux (2–3 km)	−0.10	0.15	0.85	0.79	1		
Flux (3–4 km)	0.02	0.20	0.91	0.78	0.87	1	
Flux (>4 km)	0.41	0.62	0.99	0.95	0.78	0.91	1

algorithms of *Suess* [1980] and *Martin et al.* [1987] derived from primary production and export beneath the base of the euphotic zone, respectively (Figure 4). Both the *Suess* [1980] and *Martin et al.* [1987] relationships describe flux as decreasing more rapidly with depth in the upper ocean and less rapidly with depth in the deep ocean. Disagreement between predicted and observed flux to depth is generally greatest in regions where export and primary production are larger. Disagreement is also larger in the shallow subphotic ocean (0.1–2 km) and approaches observed values with increasing depth. Within this depth range, overall disagreement is typically largest with the *Suess* [1980] relationship, which overestimates observed flux to depth by an average of 8 times and a maximum of 36 times. Here, the *Martin et al.* [1987] relationship overestimates observed flux by an average of 6 times and a maximum of 23 times. Worldwide, the *Suess* [1980] and *Martin et al.* [1987] relationships both overestimate and underestimate flux to the deep ocean (>1.5 km). The *Suess* [1980] and *Martin et al.* [1987] relationships predict flux to the deep ocean by factors

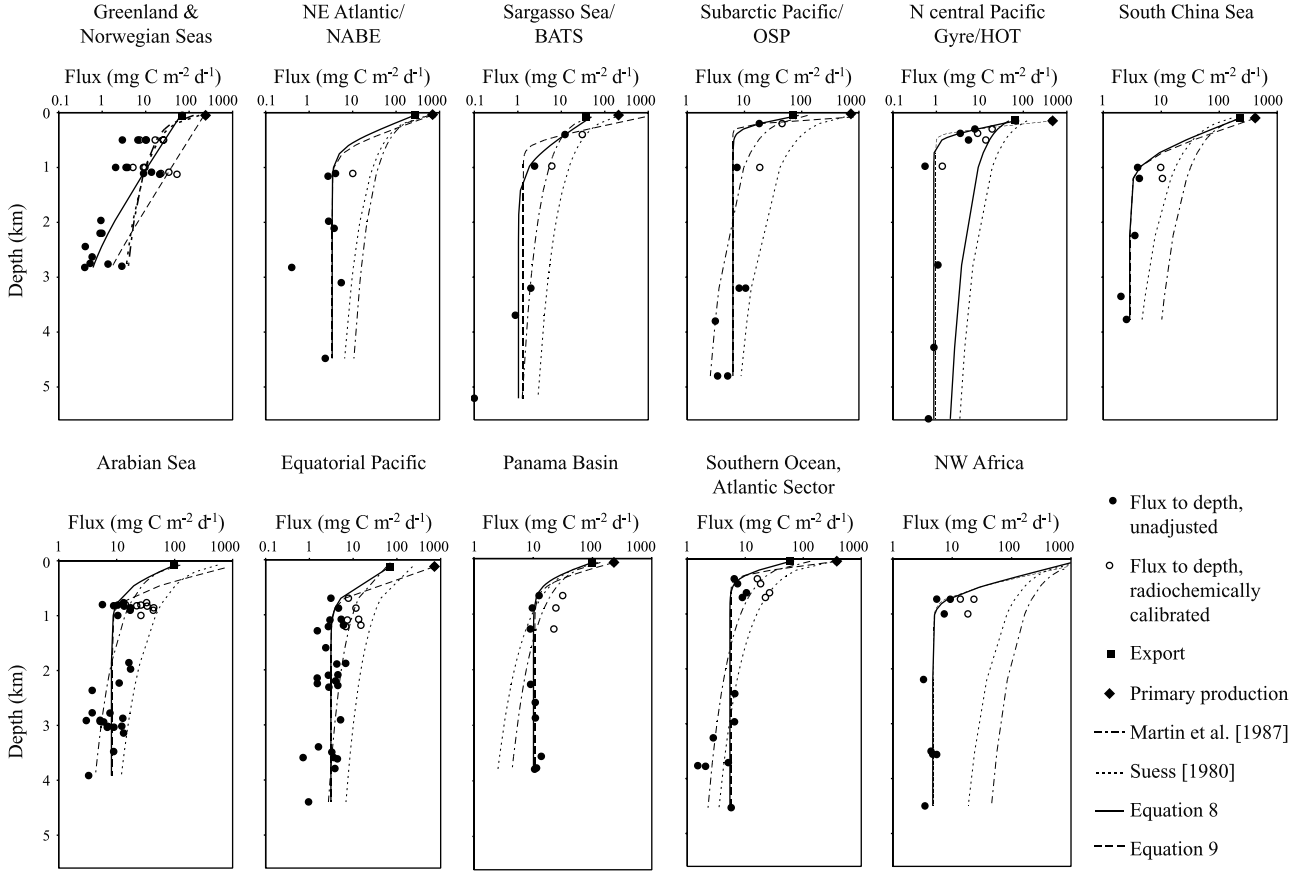

Figure 4. Regional observed (solid circles; Table 1) and radiochemically corrected (open circles) sediment-trap-based flux to depth, export (diamonds; Table 2), and primary production (squares; Table 2). Regional empirical algorithms describing the observed flux of particulate organic carbon to depth (equations (8), solid black line, and (9), dashed black line) are compared to those of *Martin et al.* [1987] (solid red line) and *Suess* [1980] (dashed red line).

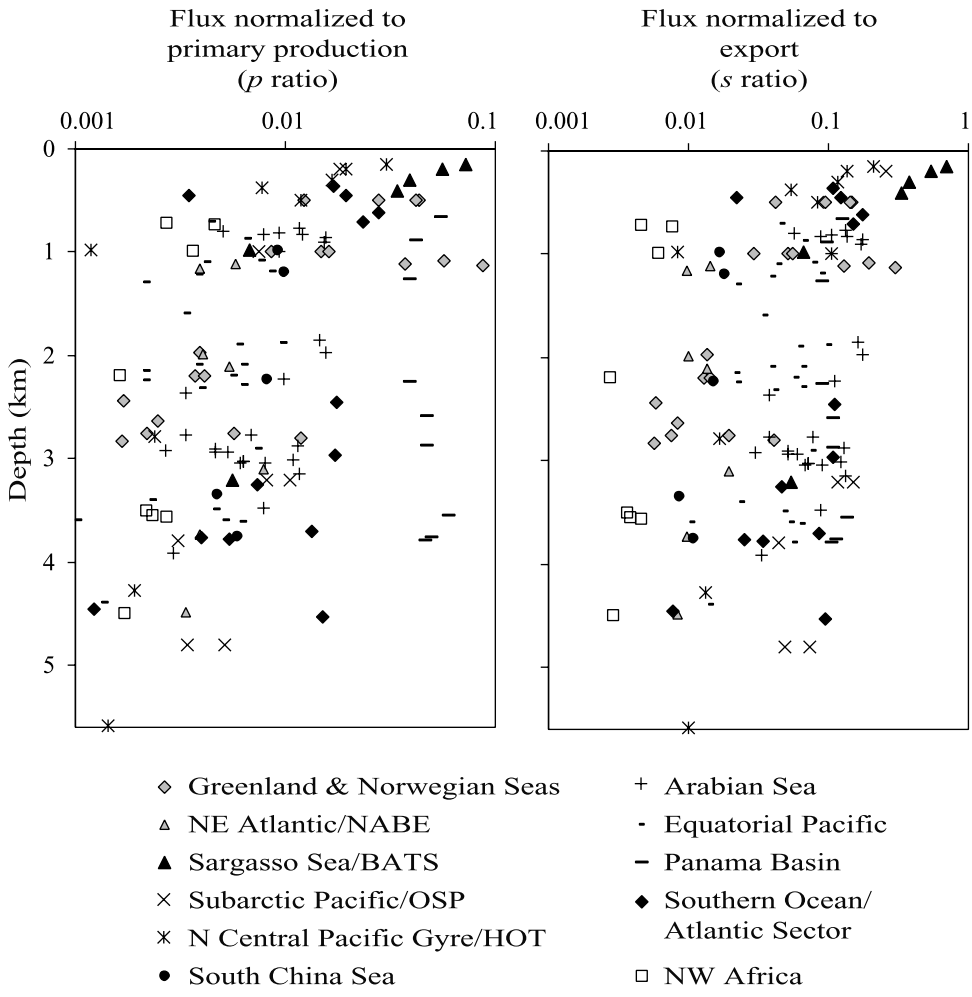

Figure 5. Observed flux to depth normalized to (a) primary production (p ratio: flux/primary production) and (b) export (s ratio: flux/export) for the major time series, JGOFS, and other oceanographic studies.

ranging from 0.2 to 6 (3.1 average) and from 0.4 to 14 (3.3 average) times observed values, respectively.

[24] The *Martin et al.* [1987] relationship predicts observed flux to depth well in some regions (Arabian Sea, Southern Ocean/Atlantic sector, and subarctic Pacific/OSP) and overestimates flux to depth in other regions studied. In regions with export values >200 mg C m^{-2} d^{-2} (NW Africa, South China Sea NE, and Atlantic/NABE), disagreement is larger. Here, predictions range between 5 and 14 times the observed values, increasing with increasing export. These disagreements suggest that organic carbon flux varies less with depth in the deep ocean than predicted by the *Martin et al.* [1987] relationship. Furthermore, in all regions, the use of the *Martin et al.* [1987] relationship with a variable exponent (instead of a fixed −0.858) underestimates observed flux to depths greater than 2 km. This implies that the use of a power law equation to describe flux to depth may overestimate the rate of change of flux with depth in the deep ocean. The inaccuracy of flux to depth exhibited by the *Martin et al.* [1987] and *Suess* [1980] relationships is probably due, in part, to the refinement of POC export and primary production methodologies over the past two decades.

4.3. Storage Efficiency p and s Ratios

[25] In order to compare flux of organic carbon between ocean regions, flux to depth is normalized to local primary production and export:

$$p_{\text{ratio}}(z) = \frac{C_{\text{flux}}(z)}{C_{\text{prod}}}, \tag{3}$$

$$s_{\text{ratio}}(z) = \frac{C_{\text{flux}}(z)}{C_{\text{export}}}. \tag{4}$$

The p and s ratios describe the vertical transport of organic carbon normalized relative to surface water primary production and export, respectively (Figure 5). These ratios gauge the efficiency of the retention of sinking organic carbon, the storage efficiency, within the deep ocean.

[26] In general, different ocean regions exhibit different groupings of p and s ratios. These groupings are more easily distinguished with s ratios than with p ratios. Large storage efficiencies of exported carbon (s ratios) are found in the Panama Basin, subarctic Pacific/OSP, Arabian Sea,

and Southern Ocean/Atlantic sector, regions. The NW Africa, north central Pacific gyre/HOT, NE Atlantic/NABE, and South China Sea regions commonly exhibit low exported carbon storage efficiencies. Fluxes per unit of carbon produced during primary production (p ratios) are largest in the Panama Basin, Southern Ocean/Atlantic sector, and Arabian Sea regions. Smaller storage efficiencies of carbon derived from primary production are found in the NW Africa, north central Pacific gyre/HOT, and NE Atlantic/NABE regions. Worldwide, the fraction of carbon fluxed to the deep ocean (>1.5 km) ranges from 0.10 to 8.8% (1.1% average) of primary production and from 0.28 to 30% (5.7% average) of export.

[27] There is little direct relationship between primary production and export and corresponding p and s ratios. Correlations between primary production or export and the regional p and s ratios are poor (all $r^2 < 0.5$). Overall, p and s ratios tend to be larger at regions with larger rates of primary production and export, suggesting that flux to depth may be more efficient during periods of low primary production and export.

4.4. Regional Empirical Algorithms

[28] The flux of POM to depth is mediated by complex physical and biological interactions that are not well understood. These interactions control the depth-dependent rates of POM sinking and remineralization. In order to better relate flux to depth to the relevant controls, we propose describing flux to depth using a minimum of parameters that include sinking and remineralization rates. Thus, flux to depth (z) can be described by the exponential equation:

$$C_{\text{flux}} = C_{\text{flux}(z_0)} e^{-\left(\frac{D}{W}\right)z}, \tag{5}$$

where D is the instantaneous rate of decay and W is the sinking rate, both in the same units of time [*Banse*, 1990, 1994].

[29] POM fluxing to depth is composed of many individual particles with a continuum of individual decay and sinking rates. As POM sinks, labile organic fractions are remineralized rapidly, allowing refractory material to become more important with depth [*Asper and Smith*, 1999; *Bishop*, 1989]. We recognize both labile and refractory fractions of sinking POM and approximate this process by modifying (5) to describe flux as the sum of two fractions of POM (s_1 and s_2), with decay rates (D_1 and D_2) and sinking rates (W_1 and W_2) normalized to export (equation (4)):

$$s(z) = s_1 e^{-\left(\frac{D_1}{W_1}\right)z} + s_2 e^{-\left(\frac{D_2}{W_2}\right)z}. \tag{6}$$

We rely on several assumptions to minimize the number of parameters needed to describe this process. Flux to depth typically decreases rapidly with increasing depth in the upper ocean. The magnitude of change of flux with increasing depth is greatly diminished in the deep ocean relative to the upper ocean. We assume that the rapid upper ocean decrease of flux to depth constitutes the rapid decay of fresh labile organic material and the near-constant fluxes approached in the deep ocean correspond to rapidly sinking organic material and/or the refractive resistance organic material to regeneration. Hence we approximate flux to depth where a fraction of POM sinks quickly or remineralizes slowly enough that decay is essentially zero (when D_2 approaches zero or W_2 approaches infinity) and (6) reduces to

$$s(z) = s_1 e^{-\left(\frac{D_1}{W_1}\right)z} + s_2. \tag{7}$$

For simplicity, we define $k_s = (D_1/W_1)\ \text{m}^{-1}$ and rewrite (7):

$$s(z) = s_1 e^{-k_s z} + s_2. \tag{8}$$

Equation (8) describes the relationship between export and flux to depth in various oceanographic regions. To describe the relationship between primary production and flux to depth, we substitute the p ratio (equation (3)) for the s ratio in (6), (7), and (8), yielding

$$p(z) = p_1 e^{-k_p z} + p_2. \tag{9}$$

The parameter k_p is defined in a similar manner to k_s. Limitations of this approximation of the flux to depth process include decay and sinking rates, which change with depth (i.e., a variable k with depth). This approximation may be insensitive to gradual decreases in the rate of flux with increasing depth, as observed in the deep ocean [*Martin et al.*, 1987; *Suess*, 1980]. The use of constant depth-independent terms (p_2 and s_2) is based on our regional analysis, which indicates that flux in the deep ocean increases with depth almost as often as it decreases with depth (Table 2).

[30] The results of the exponential fits of (8) and (9) applied to observed and radiochemically corrected regional sediment-trap-derived flux to depth, export, and primary production rate estimates are described in Tables 6a and 6b and Figures 4 and 6. These equations typically predict flux to the deep ocean within 20% of the average observed values. The p_2 and s_2 parameters describe the more rapidly sinking and/or more refractive portions of flux to the deep ocean and sediment surface. These parameters generally approximate minimum p and s ratios. The p_2 refractive/rapidly sinking fractions of primary production are above average in the Panama Basin and Southern Ocean/Atlantic sector regions. The s_2 refractive/rapidly sinking portions of export are above average in the Panama Basin, Southern Ocean/Atlantic sector, Subarctic Pacific/OSP, and Arabian Sea regions. The p_2 and s_2 values indicate that from 0.21 to 4.9% (1.2% average) of primary production and from 0.37 to 11% (4.6% average) of export reaches the deep ocean (>1.5 km), similar to calculated p and s ratios.

[31] The p_1, s_1, $1/k_p$, and $1/k_s$ parameters describe the more labile and/or more slowly sinking portion of flux. Together they approximate the remineralization length scale, or e-folding depth of flux. Smaller p_1 and s_1 values decrease the portion of flux entering the ocean at depth z_0.

Table 6a. Regional Empirical Parameters Describing Particulate Organic Carbon Flux to Depth Normalized to Primary Production Using Unadjusted and Radiochemical Calibrated Sediment Trap Fluxes[a]

	Observed			Radiochemical Calibration		
	p_1	$1/k_p$, m	p_2	p_1	$1/k_p$, m	p_2
Greenland and Norwegian Seas	1.53	116	0.00440	1.00	550	0.00104
NE Atlantic/NABE	1.37	125	0.00485	1.19	223	0.00481
Sargasso Sea/BATS	1.83	221	0.0298	3.89	102	0.00617
Subarctic Pacific/OSP	10.8	29.4	0.00627	5.80	39.7	0.00813
North central Pacific gyre/HOT	61.4	36.4	0.00210	21.7	48.8	0.00259
South China Sea	1.88	157	0.00688	1.53	230	0.00779
Arabian Sea (regional average)	1.89	119	0.00747	1.52	181	0.00744
Equatorial Pacific (regional average)	3.20	107	0.00437	3.21	105	0.0109
Panama Basin	1.69	122	0.0463	1.43	170	0.0491
Southern Ocean, Atlantic sector	1.99	56.8	0.0148	1.73	70.4	0.0172
NW Africa	1.61	104	0.00238	1.44	136	0.00301

[a] See text. The e-folding length scale of remineralization is given by $1/k_p$. All r^2 values are >0.93, except for the Greenland and Norwegian Seas region. Equation: $p(z) = p_1 e^{-kpz} + p_2$.

Larger $1/k_p$ and $1/k_s$ values deepen the inflection point of the curve describing flux, below which flux approaches p_2 or s_2 values and becomes constant with depth. The net effect is to diminish the supply of carbon to the upper ocean.

[32] These parameters are poorly constrained because of a lack of and potential unreliability of flux data in the mesopelagic zone. Parameterizations are highly sensitive to whether or not upper ocean sediment trap data are deemed valid. Applying the radiochemical correction generally lowers p_1 and s_1 values and increases $1/k_p$ and $1/k_s$ values, with the net result of decreasing flux to depth in the upper ocean. In this case, parameters derived may be considered to estimate maximum flux to depth. For both the observed and radiochemically corrected flux data, values for p_2 and s_2 greater than 0.01 are only found where primary production and export are less than 400 mg C m^{-2} d^{-1} and 150 mg C m^{-2} d^{-1}, respectively. These results suggest that where primary production and export are low, a greater portion of the transported material is refractory and/or rapidly sinking.

4.5. Effect on Carbon Storage

[33] We performed a set of simulations in a one-dimensional ocean model to assess the influence of the various remineralization profiles (equations (1), (2), (8), and (9); Tables 6a and 6b) on the retention of CO_2 generated by the remineralization of POC below the photic zone. We allowed a pulse of POC to remineralize in the ocean interior according to each regional profile and simulated how long it would take for the ΣCO_2 generated at depth to be transported back up to the photic zone.

[34] The ocean model used here is described by *Caldeira et al.* [1998]. The ocean is represented by a box diffusion model [*Oeschger et al.*, 1975; *Siegenthaler*, 1983], which is essentially a one-dimensional column representing mean oceanic vertical transport. We make no attempt to simulate regional differences in ocean circulation. The diffusion coefficients for the vertical transport of dissolved matter vary with depth. The diffusion coefficients were chosen [*Caldeira et al.*, 1998] such that the change in ocean $^{14}CO_2$ inventory between 1945 and 1975 matches the estimated 1975 bomb radiocarbon inventory [*Broecker et al.*, 1995] of 305×10^{26} atoms and the modeled 1975 ocean mean and surface ocean $\Delta^{14}CO_2$ matches the basin-volume-weighted mean of the natural plus bomb $\Delta^{14}CO_2$ values measured in the Geochemical Ocean Sections Study (GEOSECS) program [*Broecker et al.*, 1985]. The $\Delta^{14}C$ is a normalized and ^{13}C-adjusted $^{14}C/^{12}C$ ratio, and $\delta^{13}C$ is a normalized $^{13}C/^{12}C$ ratio [*Broecker and Peng*, 1982]. This tuning yields a vertical eddy diffusion coefficient of 8820 m^2 yr^{-1} at the

Table 6b. Regional Empirical Parameters Describing Particulate Organic Carbon Flux to Depth Normalized to Export Using Unadjusted and Radiochemical Calibrated Sediment Trap Fluxes[a]

Region	Observed			Radiochemical Calibration		
	s_1	$1/k_s$, m	s_2	s_1	$1/k_s$, m	s_2
Greenland and Norwegian Seas	1.28	178	0.0145	1.00	529	0.00398
NE Atlantic/NABE	1.32	137	0.0121	1.14	275	0.0119
Sargasso Sea/BATS	6.55	74.1	0.00372	1.32	599	0.0112
Subarctic Pacific/OSP	2.24	77.6	0.0896	1.00	439	0.0939
North central Pacific gyre/HOT	8.15	70.9	0.0132	3.09	122	0.0149
South China Sea	1.74	177	0.0124	1.42	278	0.0135
Arabian Sea (regional average)	1.40	183	0.0813	1.10	455	0.0617
Equatorial Pacific (regional average)	2.02	167	0.0443	1.53	243	0.0832
Panama Basin	1.44	146	0.101	1.21	228	0.112
Southern Ocean, Atlantic sector	1.33	105	0.0904	1.15	167	0.0938
NW Africa	1.55	117	0.00393	1.38	153	0.00487

[a] See text. The e-folding length scale of remineralization is given by $1/k_s$. All r^2 values are >0.93, except for the Greenland and Norwegian Seas region. Equation: $s(z) = s_1 e^{-ksz} + s_2$.

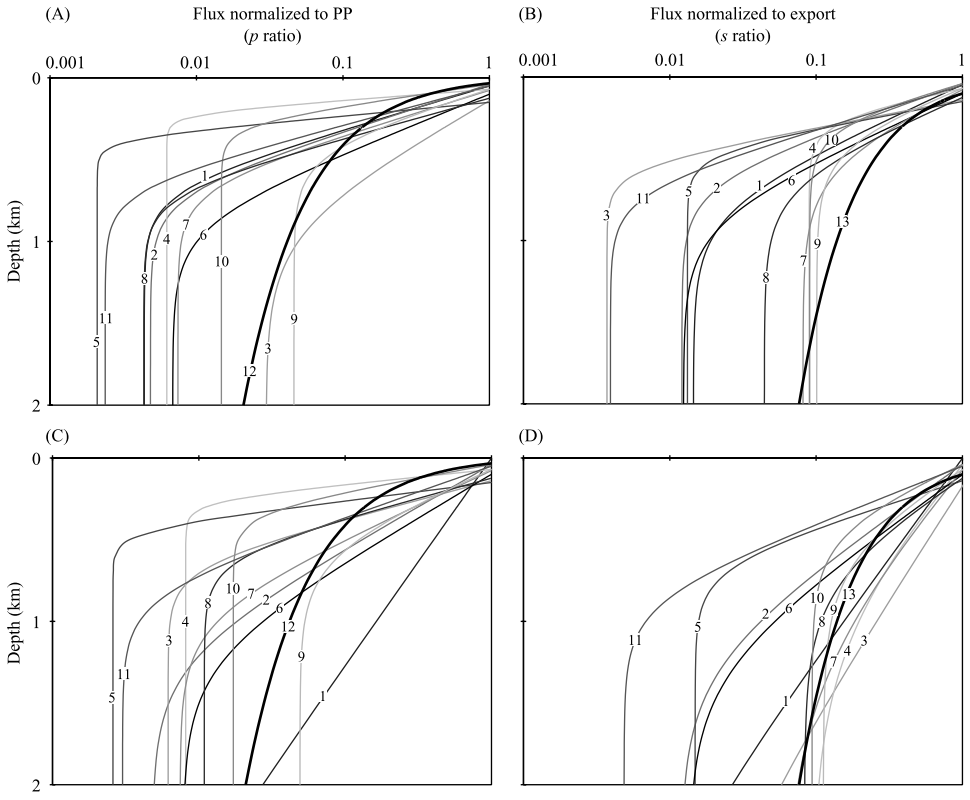

Figure 6. Regional profiles of (a and b) observed and (c and d) radiochemically corrected POC flux to depth normalized to primary production (PP) and export below the photic zone (equations (1), (2), (8), and (9); Tables 6a and 6b) for the upper 2000 m depth. Regions shown include the following: 1, Greenland and Norwegian Seas; 2, NE Atlantic/NABE; 3, Sargasso Sea/BATS; 4, Subarctic Pacific/OSP; 5, north central Pacific gyre/HOT; 6, South China Sea; 7, Arabian Sea (regional average); 8, equatorial Pacific (regional average); 9, Panama Basin; 10, Southern Ocean, Atlantic sector; and 11, NW Africa. Profiles and model results derived from the *Suess* [1980] and *Martin et al.* [1987] relationships are included for comparison (lines 12 and 13 (thick lines), respectively). See color version of this figure at back of this issue.

base of the mixed layer diminishing with an e-folding length scale of 500 m to a minimum of 2910 m^2 yr^{-1} at the ocean bottom. Similar parameter values were used in previous simulations [*Oeschger et al.*, 1975; *Siegenthaler*, 1983; *Hesshaimer et al.*, 1994].

[35] Analysis using this one-dimensional ocean model indicates that the residence time of biogenic carbon may vary up to 2 orders of magnitude depending on the regional location of carbon fixation and export. The *Suess* [1980] and *Martin et al.* [1987] relationships both yield residence times similar to the maximum of regional relationships derived in this study (Figure 7). Parameters derived from the radiochemically corrected flux to depth data typically yield longer residence times than the observed flux to depth data. Simulations based on regional profiles indicate that the residence time of POC exported below the euphotic zone in the deep ocean may span 2 orders of magnitude.

5. Conclusions

[36] We demonstrate that the commonly applied *Martin et al.* [1987] and *Suess* [1980] relationships approximate flux to depth in several locations. However, these relationships overestimate flux to depth in most ocean regions. The overestimation of flux to depth is more pronounced with the *Suess* [1980] equation. Our observations indicate that these constant power law and rational relationships used in current large-scale oceanographic models generally overestimate deepwater POC fluxes and hence underestimate particle regeneration in the water column. For a given ocean circulation model, the use of these relationships could result in unreliable estimates of new production and residence time of exported carbon in the deep ocean.

[37] We illustrate regional variability in the biological pump's ability to store carbon in the ocean below the photic zone. Flux to depth normalized to primary production and export indicates from 0.1 to 8.8% (1.1% average) of primary production and from 0.28 to 30% (5.7% average) of export enters the deep ocean (>1.5 km). The use of new region-specific empirical flux to depth algorithms, which in part parameterize the lability of settling particulate organic matter, in a one-dimensional ocean model suggests up to 2 orders of magnitude of variability in the efficiency of carbon storage in the ocean. Applying a radiochemical correction to

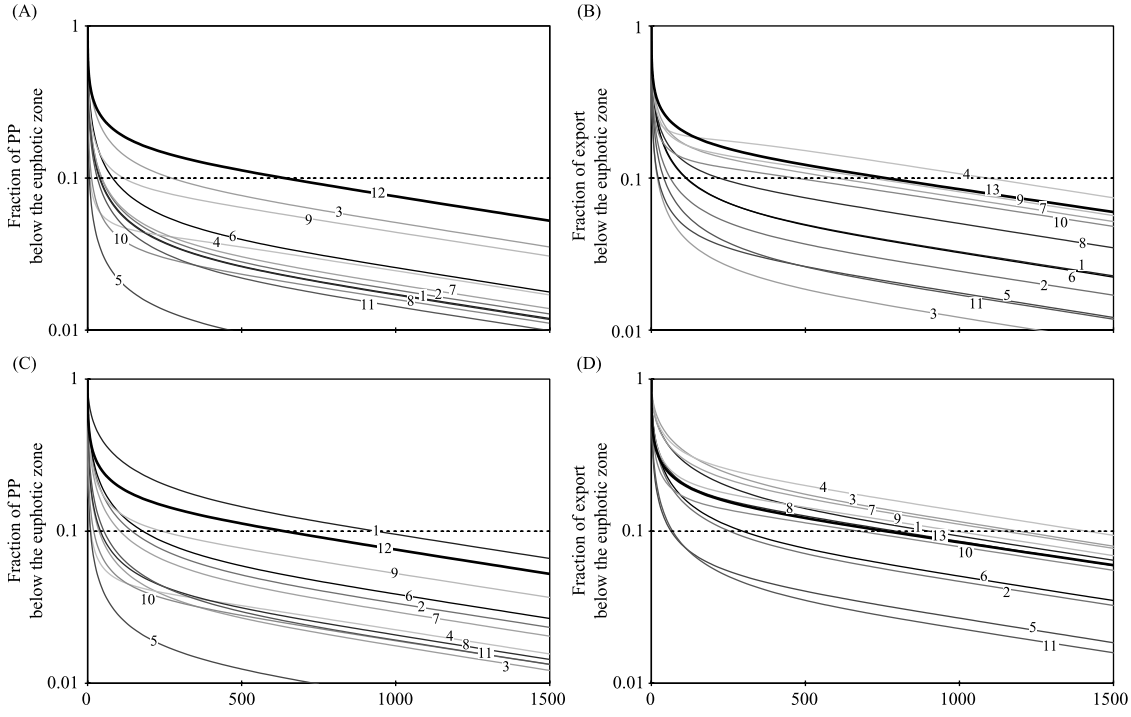

Figure 7. Predictions of (a and b) observed and (c and d) radiochemically corrected carbon storage below the photic zone using a one-dimensional ocean model (see text). Regions shown include the following: 1, Greenland and Norwegian Seas; 2, NE Atlantic/NABE; 3, Sargasso Sea/BATS; 4, Subarctic Pacific/OSP; 5, north central Pacific gyre/HOT; 6, South China Sea; 7, Arabian Sea (regional average); 8, equatorial Pacific (regional average); 9, Panama Basin; 10, Southern Ocean, Atlantic sector; and 11, NW Africa. Profiles and model results derived from the *Suess* [1980] and *Martin et al.* [1987] relationships are included for comparison (lines 12 and 13 (thick lines), respectively). See color version of this figure at back of this issue.

the observed POC flux to depth tends to lengthen remineralization length scales and subsequently increase the predicted residence time of carbon in the ocean. Global relationships between primary production and export out of the euphotic zone and flux to depth remain unclear.

[38] From our analysis it is not clear that export is any more directly related to flux to depth than is primary production. Consideration of other processes which modify the efficiency of the biological pump may improve this relationship. Modifications to the sinking flux include zooplankton swimming and excretion at depth [*Bishop*, 1989; *Bishop et al.*, 1986; *Vinogradov*, 1970], the association of fluxing material with hard parts and mineral surfaces [*Ittekkot et al.*, 1991; *Lee et al.*, 1999], variability of the mixed layer depth [*Fischer et al.*, 1996], mass sedimentation events [*DiTullio et al.*, 2000; *Kemp et al.*, 2000; *Smetacek*, 2000], plankton community structure [*Boyd and Newton*, 1999], primary production seasonality [*Berger and Wefer*, 1990; *Lampitt and Antia*, 1997], the rate of microbial decomposition [*Arnosti et al.*, 1998; *Cho and Azam*, 1988; *Laws et al.*, 2000], and non-Redfield uptake of nutrients and decomposition of organic matter [*Arrigo et al.*, 1999; *Pahlow and Riebesell*, 2000].

[39] **Acknowledgments.** We thank the following researchers for their inspiration and advice: James Bishop (Laurence Berkeley National Laboratory), Kevin Arrigo (Stanford University), and Donald Olson (RSMAS, University of Miami). This research was conducted as a portion of M. Lutz's Ph.D. dissertation and was supported by a number of sources, including the NSF ROAVERRS program, DOE Center for Research on Ocean Carbon Sequestration, Stanford University McGee Foundation, and International JGOFS Program (Ocean Biogeochemical Modeling Course, Bangalore, India).

References

Arnosti, C., B. B. Joergensen, J. Sagemann, and B. Thamdrup, Temperature dependence of microbial degradation of organic matter in marine sediments: Polysaccharide hydrolysis, oxygen consumption, and sulfate reduction, *Mar. Ecol. Prog. Ser.*, *165*, 59–70, 1998.

Arrigo, K. R., D. Worthen, A. Schnell, and M. P. Lizotte, Primary production in Southern Ocean waters, *J. Geophys. Res.*, *103*, 15,587–15,600, 1998.

Arrigo, K. R., D. H. Robinson, D. L. Worthen, R. B. Dunbar, G. R. DiTullio, M. VanWoert, and M. P. Lizotte, Phytoplankton community structure and the drawdown of nutrients and CO_2 in the Southern Ocean, *Science*, *283*, 365–367, 1999.

Asper, V. L., and W. O. Smith Jr., Particle fluxes during austral spring and summer in the southern Ross Sea, Antarctica, *J. Geophys. Res.*, *104*, 5345–5359, 1999.

Baker, E. T., H. B. Milburn, and D. A. Tennant, Field assessment of sediment trap efficiency under varying flow conditions, *J. Mar. Res.*, *46*, 573–592, 1988.

Banse, K., New views on the degradation and disposition of organic particles as collected by sediment traps in the open sea, *Deep Sea Res., Part A*, *37*, 1177–1195, 1990.

Banse, K., On the coupling of hydrography, phytoplankton, zooplankton, and settling organic particles offshore in the Arabian Sea, in *Biogeochemistry of the Arabian Sea*, edited by D. Lal, pp. 125–161, Indian Acad. of Sci., Bangalore, 1994.

Barber, R. T., J. Marra, R. C. Bidigare, L. A. Codispoti, D. Halpern, Z. Johnson, M. Latasa, R. Goericke, and S. L. Smith, Primary productivity and its regulation in the Arabian Sea during 1995, *Deep Sea Res., Part II*, *48*, 1127–1172, 2001.

Bathmann, U. V., R. Peinert, T. T. Noji, and B. V. Bodungen, Pelagic origin and fate of sedimenting particles in the Norwegian Sea, *Prog. Oceanogr.*, *24*, 117–125, 1990.

Berger, W. H., and G. Wefer, Export production: Seasonality and intermittency, and paleoceanographic implications, *Global Planet. Change*, *89*, 245–254, 1990.

Bishop, J. K. B., Regional extremes in particulate matter composition and flux: Effects on the chemistry of the ocean interior, in *Productivity of the Ocean: Present and Past*, edited by W. H. Berger, V. Smetacek, and G. Wefer, pp. 117–38, John Wiley, New York, 1989.

Bishop, J. K. B., J. C. Stepian, and P. H. Wiebe, Particle matter distributions, chemistry and flux in the Panama Basin: Response to environmental forcing, *Prog. Oceanogr.*, *17*, 1–59, 1986.

Bodungen, B. V., et al., Pelagic processes and vertical flux of particles: An overview of a long-term comparative study in the Norwegian Sea and Greenland Sea, *Geol. Rundsch.*, *84*, 11–27, 1995.

Boyd, P. W., and P. J. Harrison, Phytoplankton dynamics in the NE subarctic Pacific, *Deep Sea Res., Part II*, *46*, 2405–2432, 1999.

Boyd, P. W., and P. P. Newton, Evidence of the potential influence of planktonic community structure on the interannual variability of particulate organic carbon flux, *Deep Sea Res., Part I*, *42*, 619–639, 1995.

Boyd, P. W., and P. P. Newton, Does planktonic community structure determine downward particulate organic carbon flux in different oceanic provinces?, *Deep Sea Res., Part I*, *46*, 63–91, 1999.

Brewer, P. G., C., Goyet, G., Fredrich, Direct observation of the oceanic CO_2 increase revisited, in *Proc. Natl. Acad. Sci. U. S. A.*, *94*, 8308–8313, 1997.

Broecker, W. S., and T.-H., Peng, *Tracers in the Sea*, 690 pp., Lamont-Doherty Earth Obs., Palisades, N. Y., 1982.

Broecker, W. S., T.-H. Peng, H. G. Ostlund, and M. Stuiver, The distribution of bomb radiocarbon in the ocean, *J. Geophys. Res.*, *90*, 6925–6939, 1985.

Broecker, W. S., S. Sutherland, W. Smithie, T. H. Peng, and G. Ostlund, Oceanic radiocarbon: Separation of the bomb and natural components, *Global Biogeochem. Cycles*, *9*, 263–288, 1995.

Buesseler, K. O., Do upper-ocean sediment traps provide an accurate record of particle flux?, *Nature*, *353*, 420–423, 1991.

Buesseler, K. O., The decoupling of production and export in the surface ocean, *Global Biogeochem. Cycles*, *12*, 297–310, 1998.

Buesseler, K. O., M. P. Bacon, J. K. Cochran, and H. D. Livingston, Carbon and nitrogen export during the JGOFS North Atlantic Bloom Experiment estimated from ^{234}Th:^{238}U disequilibria, *Deep Sea Res., Part A*, *39*, 1115–1137, 1992.

Buesseler, K. O., L. Ball, J. Andrews, C. Benitez-Nelson, R. Belastock, F. Chai, and Y. Chao, Upper ocean export of particulate organic carbon in the Arabian Sea derived from thorium-234, *Deep Sea Res., Part II*, *45*, 2461–2487, 1998.

Buesseler, K. O., D. K. Steinberg, A. F. Michaels, R. J. Johnson, J. E. Andrews, J. R. Valdes, and J. F. Price, A comparison of the quantity and composition of material caught in a neutrally buoyant versus surface tethered sediment trap, *Deep Sea Res., Part I*, *47*, 169–187, 2000.

Bury, S. J., P. W. Boyd, T. Preston, G. Savidge, and N. J. P. Owens, Size-fractionated primary production and nitrogen uptake during a North Atlantic phytoplankton bloom: Implications for carbon export estimates, *Deep Sea Res., Part I*, *48*, 689–720, 2001.

Caldeira, K., G. H. Rau, and P. B. Duffy, Predicted net efflux of radiocarbon from the ocean and increase in atmospheric radiocarbon content, *Geophys. Res. Lett.*, *25*, 3811–3814, 1998.

Charette, M. A., S. B. Moran, and J. K. B. Bishop, ^{234}Th as a tracer of particulate organic carbon export in the subarctic northeast Pacific Ocean, *Deep Sea Res., Part II*, *46*, 2833–2861, 1999.

Cho, B. C., and F. Azam, Major role of bacteria in biogeochemical fluxes in the ocean's interior, *Nature*, *332*, 441–443, 1988.

Dam, H. G., M. R. Roman, and M. J. Youngbluth, Downward export of respiratory carbon and dissolved inorganic nitrogen by diel-migrant mesozooplankton at the JGOFS Bermuda time-series station, *Deep Sea Res., Part I*, *42*, 1187–1197, 1995.

Deuser, W. G., F. E. Muller-Karger, R. H. Evans, O. B. Brown, W. E. Esaias, and G. C. Feldman, Surface-ocean color and deep-ocean carbon flux: How close a connection?, *Deep-Sea Res., Part A*, *37*, 1331–1343, 1990.

DiTullio, G. R., J. M. Grebmeier, K. R. Arrigo, M. P. Lizotte, D. H. Robinson, A. Leventer, J. P. Barry, M. L. VanWoert, and R. B. Dunbar, Rapid and early export of *Phaeocystis antarctica* blooms in the Ross Sea, Antarctica, *Nature*, *404*, 595–598, 2000.

Dring, M. J., and D. H. Jewson, What does ^{14}C uptake by phytoplankton really measure?: A theoretical modelling approach, *Proc. R. Soc. London, Ser. B.*, *214*, 351–368, 1982.

Druffel, E. R. M., S. Griffin, J. E. Bauer, D. M. Wolgast, and X. C. Wang, Distribution of particulate organic carbon and radiocarbon in the water column from the upper slope to the abyssal NE Pacific ocean, *Deep Sea Res., Part II*, *45*, 667–687, 1998.

Dymond, J., and R. Collier, Biogenic particle fluxes in the equatorial Pacific: Evidence for both high and low productivity during the 1982–1983 El Niño, *Global Biogeochem. Cycles*, *2*, 129–137, 1988.

Dymond, J., R. Collier, J. McManus, S. Honjo, and S. Manganini, Can the aluminum and titanium contents of ocean sediments be used to determine the paleoproductivity of the oceans?, *Paleoceanography*, *12*, 586–593, 1997.

Emerson, S., P. Quay, D. Karl, C. Winn, L. Tupas, and M. Landry, Experimental determination of the organic carbon flux from open-ocean surface waters, *Nature*, *389*, 951–954, 1997.

Eppley, R., and B. Peterson, Particulate organic matter flux and planktonic new production in the deep ocean, *Nature*, *282*, 677–680, 1979.

Fischer, G., B. Donner, B. Davenport, V. Ratmeyer, and G. Wefer, Distinct year-to-year particle variations off Cape Blanc during 1988–1991: Relation to δ^{18}0-deduced sea-surface temperature and trade winds, *J. Mar. Res.*, *54*, 73–98, 1996.

Fischer, G., V. Ratmeyer, and G. Wefer, Organic carbon fluxes in the Atlantic and the Southern Ocean: relationship to primary production compiled from satellite radiometer data, *Deep-Sea Res., Part II*, *47*, 1961–1997, 2000.

Gardner, W. D., Sediment trap sampling in surface waters, in *The Changing Ocean Carbon Cycle*, edited by R. B. Hanson, H. W. Ducklow, and J. G. Field, 514 pp., Cambridge University Press, New York, 2000.

Grasshoff, K., K. Kremling, and M. Ehrhardt (Eds.), *Methods of Seawater Analysis*, 600 pp., John Wiley, New York, 1999.

Gust, G., and H. P. Kozerski, In situ sinking-particle flux from collection rates of cylindrical traps, *Mar. Ecol. Prog. Ser.*, *208*, 93–106, 2000.

Gust, G., R. H. Byrne, R. E. Bernstein, P. R. Betzer, and W. Bowles, Particle fluxes and moving fluids: Experience from synchronous trap collections in the Sargasso Sea, *Deep Sea Res., Part A*, *39*, 1071–1083, 1992.

Gust, G., A. F. Michaels, R. Johnson, W. G. Deuser, and W. Bowles, Mooring line motions and sediment trap hydromechanics: In situ intercomparison of three common deployment designs, *Deep Sea Res., Part I*, *41*, 831–857, 1994.

Haake, B., V. Ittekkot, T. Rixen, V. Ramaswamy, R. R. Nair, and W. B. Curry, Seasonality and interannual variability of particle fluxes to the deep Arabian Sea, *Deep Sea Res., Part I*, *40*, 1323–1344, 1993.

Hebbeln, D., Flux of ice-rafted detritus from sea ice in the Fram Strait, *Deep Sea Res., Part II*, *47*, 1773–1790, 2000.

Hebbeln, D., M. Marchant, and G. Wefer, Seasonal variations of the particle flux in the Peru-Chile current at 30°S under "normal" and El Niño conditions, *Deep Sea Res., Part II*, *47*, 2101–2128, 2000.

Hedges, J. I., F. S. Hu, A. H. Devol, H. E. Hartnett, E. Tsamakis, and R. G. Keil, Sedimentary organic matter preservation: A test for selective degradation under oxic conditions, *Am. J. Sci.*, *299*, 529–555, 1999.

Hesshaimer, V., M. Heimann, and I. Levin, Radiocarbon evidence for a smaller oceanic carbon dioxide sink than previously believed, *Nature*, *370*, 201–203, 1994.

Honjo, S., Material fluxes and modes of sedimentation in the mesopelagic and bathypelagic zones, *J. Mar. Res.*, *38*, 53–97, 1980.

Honjo, S., Seasonality and interaction of biogenic and lithogenic particulate flux at the Panama Basin, *Science*, *218*, 883–884, 1982.

Honjo, S., Ocean particle and fluxes of material to the interior of the deep ocean: The azoic theory 120 years later, in *Facets of Modern Biogeochemistry*, edited by V. Ittekkot et al., pp. 62–73, Springer-Verlag, New York, 1990.

Honjo, S., and S. J. Manganini, Annual biogenic particle fluxes to the interior of the North Atlantic Ocean: Studied at 34°N 21°W and 4S°N 21°W, *Deep Sea Res., Part II*, *40*, 587–607, 1993.

Honjo, S., S. J. Manganini, and J. J. Cole, Sedimentation of biogenic matter in the deep ocean, *Deep Sea Res., Part A*, *29*, 609–625, 1982.

Honjo, S., S. J. Manganini, A. Karowe, and B. L. Woodward, *Particle fluxes, North-Eastern Nordic Seas: 1983–1986*, *Rep. WHOI-87-17*, 84 pp., Woods Hole Oceanogr. Inst., Woods Hole, Mass., 1987.

Honjo, S., J. Dymond, R. Collier, and S. J. Manganini, Export production of particles to the interior of the Equatorial Pacific Ocean during the 1992 EqPac experiment, *Deep Sea Res., Part II*, *42*, 831–870, 1995.

Honjo, S., J. Dymond, W. Prel, and V. Ittekkot, Monsoon-controlled export fluxes to the interior of the Arabian Sea, *Deep Sea Res., Part II*, *46*, 1859–1902, 1999.

Honjo, S., R. Francois, S. Manganini, J. Dymond, and R. Collier, Particle fluxes to the interior of the Southern Ocean in the Western Pacific sector along 170°W, *Deep Sea Res., Part II*, *47*, 3521–3548, 2000.

Huang, Y., Distribution characteristics of chlorophyll a and estimation of primary productivity in the waters around Nansha Islands, in *Proceedings on Marine Biology of the South China Sea*, edited by X. Gongzhao and B. Morton, pp. 261–276, Hong Kong Univ. Press, Hong Kong, 1988.

Huang, Y., M. Chen, F. Chen, Y. Qiu, Y. Xie, L. Huang, S. Chen and H. Wang, and Hankui, Particle dynamics in euphotic zone, 3, The stratified structure and export production in the euphotic zone of the Nansha sea area, in *Isotope Marine Chemistry of Nansha Islands Waters*, pp. 134–144, China Ocean Press, Beijing, 1996.

Huntsman, S. A., and R. T. Barber, Primary production off northwest Africa: Relationship to wind and nutrient conditions, *Deep Sea Res.*, *24*, 25–33, 1977.

Ittekkot, V., R. Nair, S. Honjo, V. Ramaswamy, M. Bartsch, S. J. Manganini, and B. N. Desai, Enhanced particle fluxes in Bay of Bengal induced by injection of water, *Nature*, *351*, 385–387, 1991.

Jewell, P. W., Mass-balance models of Ekman transport and nutrient fluxes in coastal upwelling zones, *Global Biogeochem. Cycles*, *8*, 165–177, 1994.

Jianfang, C., Z. Lianfu, M. G. Wiesner, C. Ronghua, Z. Yulong, and K. H. Wong, Estimations of primary productivity and export production in the South China Sea based on sediment trap experiments, *Chin. Sci. Bull.*, *43*, 585–586, 1998.

Jurg, B., Towards a new generation of sediment traps and a better measurement/understanding of settling particle flux in lakes and oceans: A hydrodynamical protocol, *Aquat. Sci.*, *58*, 283–296, 1996.

Karl, D. M., and G. A. Knauer, Swimmers: A recapitulation of the problem and a potential solution, *Oceanography*, *2*, 32–35, 1989.

Karl, D. M., J. R. Christian, J. E. Dore, D. V. Hebel, R. M. Letelier, L. M. Tupas, and C. D. Winn, Seasonal and interannual variability in primary production and particle flux at Station ALOHA, *Deep Sea Res., Part II*, *43*, 539–568, 1996.

Kemp, A. E. S., J. Pike, R. B. Pearce, and C. B. Lange, The "Fall dump": A new perspective on the role of a "shade flora" in the annual cycle of diatom production and export flux, *Deep Sea Res., Part II*, *47*, 2129–2154, 2000.

Kempe, S., H. Knaack, Vertical particle flux in the western Pacific below the north equatorial current and the equatorial counter current, in *Particle Flux in the Ocean*, edited by V. Ittekkot et al., *SCOPE*, *57*, 313–324, 1996.

Kim, G. N., N. Hussain, and T. M. Church, How accurate are the ^{234}Th based particulate residence times in the ocean?, *Geophys. Res. Lett.*, *26*, 619–622, 1999.

Knauer, G. A., J. H. Martin and D. M. Karl, The flux of particulate organic matter out of the euphotic zone, in *Global Ocean Flux Study: Proceedings of a Workshop*, pp. 136–150, Natl. Acad. Press, Washington, D. C., 1984a.

Knauer, G. A., D. M. Karl, J. H. Martin, and C. N. Hunter, In situ effects of selected preservatives on total carbon, nitrogen and metals collected in sediment traps, *J. Mar. Res.*, *42*, 445–462, 1984b.

Kurz, K. D., and E. Maier-Reimer, Iron fertilization of the Austral Ocean: The Hamburg Model assessment, *Global Biogeochem. Cycles*, *7*, 229–244, 1993.

Lampitt, R. S., and A. N. Antia, Particle flux in deep seas: Regional characteristics and temporal variability, *Deep Sea Res., Part I*, *44*, 1377–1403, 1997.

Laws, E. A., P. G. Falkowski, W. O. Smith, H. Ducklow, and J. J. McCarthy, Temperature effects on export production in the open ocean, *Global Biogeochem. Cycles*, *14*, 1231–1246, 2000.

Lee, C., S. G. Wakeham, and J. I. Hedges, The measurement of oceanic particles flux: Are "swimmers" a problem?, *Oceanography*, *1*, 34–36, 1988.

Lee, C., et al., Particulate organic carbon fluxes: compilation of results from the 1995 US JGOFS Arabian Sea Process Study, *Deep Sea Res., Part II*, *45*, 2489–2501, 1998.

Lee, C., R. A. Armstrong, J. I. Hedges, S. Honjo, and S. G. Wakeham, Remineralization of particulate organic carbon in the deep ocean: A mechanistic model of transport and protection by inorganic minerals (abstract), *Eos Trans. AGU*, *80*(49), Ocean Sci. Meet. Suppl., OS249, 1999.

Lee, T., E. Barg, D. Lal, and F. Azam, Bacterial scavenging of ^{234}Th in surface ocean waters, *Mar. Ecol. Prog. Ser.*, *96*, 109–116, 1993.

Longhurst, A. R., and W. G. Harrison, Vertical nitrogen flux from the oceanic photic zone by diel migrant zooplankton and nekton, *Deep Sea Res., Part A*, *35*, 881–889, 1988.

Lorenzen, C. J., F. R. Shuman, and J. T. Bennett, In situ calibration of a sediment trap, *Limnol. Oceanogr.*, *26*, 580–585, 1981.

Macintyre, S., A. L. Alldredge, and C. C. Gotschalk, Accumulation of marine snow at density discontinuities in the water column, *Limnol. Oceanogr.*, *40*, 449–468, 1995.

Martin, J. H., G. A. Knauer, D. M. Karl, and W. W. Broenkow, VERTEX: Carbon cycling in the northeast Pacific, *Deep Sea Res., Part A*, *34*, 267–285, 1987.

Michaels, A. F., M. W. Silver, M. M. Gowing, and G. A. Knauer, Cryptic zooplankton "swimmers" in the upper ocean sediment traps, *Deep Sea Res., Part A*, *37*, 1285–1296, 1990.

Michaels, A. F., N. R. Bates, K. O. Buesseler, C. A. Carlson, and A. H. Knap, Carbon-cycle imbalances in the Sargasso Sea, *Nature*, *372*, 537–539, 1994.

Minas, H. J., M. Minas, and T. T. Packard, Productivity in upwelling areas deduced from hydrographic and chemical fields, *Limnol. Oceanogr.*, *31*, 1182–1206, 1986.

Murray, J. W., J. Young, J. Newton, J. Dunne, T. Chapin, B. Paul, and J. J. McCarthy, Export flux of particulate organic carbon from the central equatorial Pacific determined using a combined drifting trap: ^{234}Th approach, *Deep Sea Res., Part II*, *43*, 1095–1132, 1996.

Newton, P. P., R. S. Lampitt, T. D. Jickells, P. King, and C. Boutle, Temporal and spatial variability of biogenic particle fluxes during the JGOFS northeast Atlantic process studies at 47′N 20′W, *Deep Sea Res., Part II*, *41*, 1617–1642, 1994.

Oeschger, H., U. Siegenthaler, U. Schotterer, and A. Gugelmann, A box diffusion model to study the carbon dioxide exchange in nature, *Tellus, Ser. B*, *27*, 168–192, 1975.

Paerl, H. W., Coastal eutrophication and harmful algal blooms: Importance of atmospheric deposition and groundwater as "new" nitrogen and other nutrient sources, *Limnol. Oceanogr.*, *42*, 1154–1165, 1997.

Pahlow, M., and U. Riebesell, Temporal trends in deep ocean Redfield ratios, *Science*, *287*, 831–833, 2000.

Petsch, S. T., and R. A. Berner, Coupling the geochemical cycles of C, P, Fe, and S: The effect on atmospheric O_2 and the isotopic records of carbon and sulfur, *Am. J. Sci.*, *298*, 246–262, 1998.

Pudsey, C. J., and P. King, Particle fluxes, benthic processes and the palaeoenvironmental record in the northern Weddell Sea, *Deep Sea Res., Part I*, *44*, 1841–1876, 1997.

Quay, P., Was a carbon balance measured in the equatorial Pacific during JGOFS?, *Deep Sea Res., Part II*, *44*, 1765–1781, 1997.

Sakshaug, E., A. Bricaud, Y. Dandonneau, P. G. Falkowski, D. A. Kiefer, L. Legendre, A. Morel, J. Parslow, and M. Takahashi, Parameters of photosynthesis: Definitions, theory and interpretation of results, *J. Plankton Res.*, *19*, 1637–1670, 1997.

Sambrotto, R. N., and B. J. Mace, Coupling of biological and physical regimes across the Antarctic Polar Front as reflected by nitrogen production and recycling, *Deep Sea Res., Part II*, *47*, 3339–3367, 2000.

Sarmiento, J. L., and C. Le Quere, Oceanic carbon dioxide uptake in a model of century-scale global warming, *Science*, *274*, 1346–1350, 1996.

Sarmiento, J. L., T. M. C. Hughes, R. J. Stouffer, and S. Manabe, Simulated response of the ocean carbon cycle to anthropogenic climate warming, *Nature*, *393*, 245–249, 1998.

Scholten, J. C., et al., Trapping efficiencies of sediment traps from the deep eastern North Atlantic, *Deep Sea Res., Part II*, *48*, 2283–2408, 2001.

Siegel, D. A., and W. G. Deuser, Trajectories of sinking particles in the Sargasso Sea: Modeling of statistical funnels above deep-ocean sediment traps, *Deep Sea Res., Part II*, *44*, 1519–1541, 1997.

Siegel, D. A., T. C. Granata, A. F. Michaels, and T. D. Dickey, Mesoscale eddy diffusion, particle sinking, and the interpretation of sediment trap data, *J. Geophys. Res.*, *95*, 5305–5311, 1990.

Siegenthaler, U., Uptake of excess CO_2 by an outcrop-diffusion model of the ocean, *J. Geophys. Res.*, *88*, 3599–3608, 1983.

Sigman, D. M., D. C. McCorkle, and W. R. Martin, The calcite lysocline as a constraint on glacial/interglacial low-latitude production changes, *Global Biogeochem. Cycles*, *12*, 409–427, 1998.

Six, K. D., and E. Maier-Reimer, Effects of plankton dynamics on seasonal carbon fluxes in an ocean general circulation model, *Global Biogeochem. Cycles*, *10*, 559–583, 1996.

Smetacek, V., The giant diatom dump, *Nature*, *406*, 574–575, 2000.

Soltwedel, T., Meiobenthos distribution pattern in the tropical East Atlantic: Indication for fractionated sedimentation of organic matter to the sea floor?, *Mar. Biol.*, *129*, 747–756, 1997.

Stoll, M. H. C., H. M. Van Aken, H. J. W. De Baar, and C. J. De Boer, Meridional carbon dioxide transport in the northern North Atlantic, *Mar. Chem.*, *55*, 205–216, 1996.

Suess, E., Particulate organic carbon flux in the oceans: Surface productivity and oxygen utilization, *Nature*, *288*, 260–263, 1980.

Takahashi, K., Opal particle flux in the subarctic Pacific and Bering Sea and sidocoenosis preservation hypothesis, in *Global Fluxes of Carbon and Its Related Substances in the Coastal, Sea-Ocean-Atmosphere System: Pro-*

ceedings of the 1994 Sapporo IGBP Symposium, Hokkaido University, Sapporo Hokkaido, Japan, edited by S. Tsunogai, M&J Int., Yokohama, Japan, 1995.

Tyrell, T., The relative influences of nitrogen and phosphorus on oceanic primary production, *Nature*, *400*, 525–531, 1999.

Usbeck, R., Modeling of marine biogeochemical cycles with an emphasis on vertical particle fluxes, *Rep. Polar Res.*, *332*, 105 pp., 1999.

VanderLoeff, M. M. R., J. Friedrich, and U. V. Bathmann, Carbon export during the spring bloom at the Antarctic Polar Front, determined with the natural tracer ^{234}Th, *Deep Sea Res., Part II*, *44*, 457–478, 1997.

Vinogradov, M. E., *Vertical Distribution of the Oceanic Zooplankton*, translated from Russian by A. Mercado and J. Salkind, 339 pp., Isr. Program for Sci. Transl., Jerusalem, 1970.

Walsh, I., K. Fischer, D. Murray, and J. Dymond, Evidence for resuspension of rebound particles from near-bottom sediment traps, *Deep Sea. Res., Part A*, *35*, 59–70, 1988.

Wefer, G., and G. Fischer, Annual primary production and export flux in the Southern Ocean from sediment trap data, *Mar. Chem.*, *35*, 597–613, 1991.

Wefer, G., and G. Fischer, Seasonal patterns of vertical particle flux in the equatorial and coastal upwelling areas of the eastern Atlantic, *Deep Sea Res., Part I*, *40*, 1613–1645, 1993.

Wefer, G., G. Fischer, D. Fuetterer, and R. Gersonde, Seasonal particle flux in the Bransfield Strait, Antarctica, *Deep Sea Res., Part A*, *35*, 891–898, 1988.

Wei, C., and J. W. Murray, Temporal variations of ^{234}Th activity in the water column of Dabob Bay: Particle scavenging, *Limnol. Oceanogr.*, *37*, 296–314, 1992.

Wiesner, M. G., L. Zheng, H. K. Wong, Y. Wang and W. Chen, Fluxes of particulate matter in the South China Sea, in *Particle Flux in the Ocean*, edited by V. Ittekkot et al., *SCOPE*, *57*, 293–312, 1996.

Wong, C. S., F. A. Whitney, D. W. Crawford, K. Iseki, R. J. Matear, W. K. Johnson, J. S. Page, and D. Timothy, Seasonal and interannual variability in particle fluxes of carbon, nitrogen and silicon from time series of sediment traps at Ocean Station P, 1982–1993: Relationship to changes in subarctic primary productivity, *Deep Sea Res., Part II*, *46*, 2735–2760, 1999.

Yu, E. F., R. Francois, M. P. Bacon, S. Honjo, A. P. Fleer, S. J. Manganini, M. M. R. VanderLoeff, and V. Ittekot, Trapping efficiency of bottom-tethered sediment estimated from intercepted fluxes of ^{230}Th and ^{231}Pa, *Deep Sea Res., Part I*, *48*, 865–889, 2001.

K. Caldeira, Climate Modeling Group, Lawrence Livermore National Laboratory, 7000 East Avenue, L-103, Livermore, CA 94550, USA. (kenc@llnl.gov)

R. Dunbar and M. Lutz, Department of Geological and Environmental Science, Stanford University, Stanford, CA 94305-2115, USA. (lutz@pangea.stanford.edu; dunbar@pangea.stanford.edu)

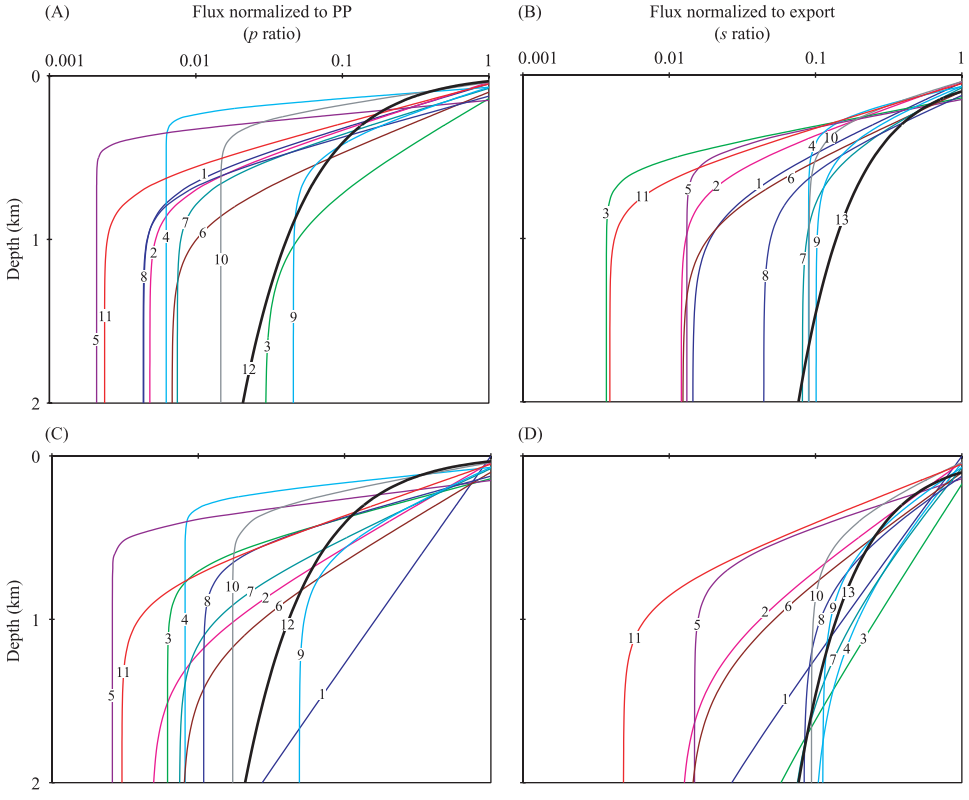

Figure 6. Regional profiles of (a and b) observed and (c and d) radiochemically corrected POC flux to depth normalized to primary production (PP) and export below the photic zone (equations (1), (2), (8), and (9); Tables 6a and 6b) for the upper 2000 m depth. Regions shown include the following: 1, Greenland and Norwegian Seas; 2, NE Atlantic/NABE; 3, Sargasso Sea/BATS; 4, Subarctic Pacific/OSP; 5, north central Pacific gyre/HOT; 6, South China Sea; 7, Arabian Sea (regional average); 8, equatorial Pacific (regional average); 9, Panama Basin; 10, Southern Ocean, Atlantic sector; and 11, NW Africa. Profiles and model results derived from the *Suess* [1980] and *Martin et al.* [1987] relationships are included for comparison (lines 12 and 13 (thick lines), respectively).

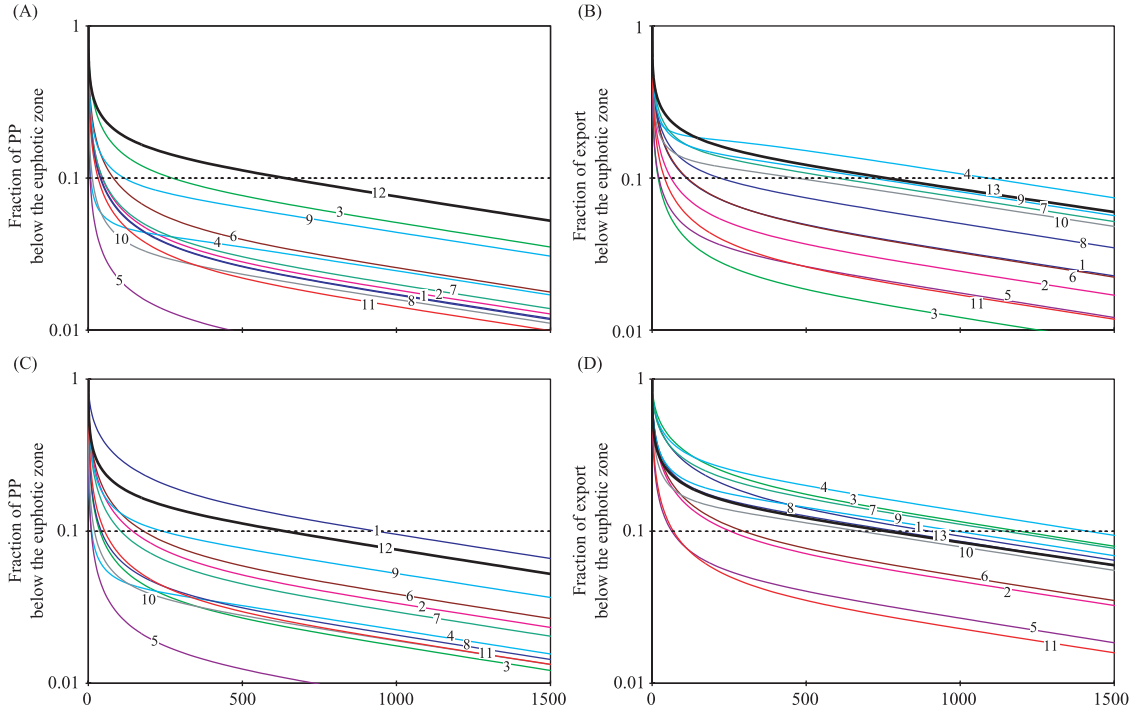

Figure 7. Predictions of (a and b) observed and (c and d) radiochemically corrected carbon storage below the photic zone using a one-dimensional ocean model (see text). Regions shown include the following: 1, Greenland and Norwegian Seas; 2, NE Atlantic/NABE; 3, Sargasso Sea/BATS; 4, Subarctic Pacific/OSP; 5, north central Pacific gyre/HOT; 6, South China Sea; 7, Arabian Sea (regional average); 8, equatorial Pacific (regional average); 9, Panama Basin; 10, Southern Ocean, Atlantic sector; and 11, NW Africa. Profiles and model results derived from the *Suess* [1980] and *Martin et al.* [1987] relationships are included for comparison (lines 12 and 13 (thick lines), respectively).